Taylor & Francis
Taylor & Francis Group

Check for updates

Marine algal antagonists targeting 3CL protease and spike glycoprotein of SARS-CoV-2: a computational approach for anti-COVID-19 drug discovery

Malaisamy Arunkumar[a,b]*, Sathaiah Gunaseelan[c]*, Manikka Kubendran Aravind[a]*, Verma Mohankumar[c], Patra Anupam[b], Muniyasamy Harikrishnan[d], Ayyanar Siva[d], Balasubramaniem Ashokkumar[a] and Perumal Varalakshmi[c] [iD]

[a]Department of Genetic Engineering, School of Biotechnology, Madurai Kamaraj University, Madurai, Tamil Nadu, India; [b]International Centre for Genetic Engineering and Biotechnology (ICGEB), Transcription Regulation Group, New Delhi, India; [c]Department of Molecular Microbiology, School of Biotechnology, Madurai Kamaraj University, Madurai, Tamil Nadu, India; [d]Supramolecular and Organometallic Chemistry Lab, Department of Inorganic Chemistry, School of Chemistry, Madurai Kamaraj University, Madurai, Tamil Nadu, India

Communicated by Ramaswamy H. Sarma

ABSTRACT

The COVID-19 pandemic has severely destructed human life worldwide, with no suitable treatment until now. SARS-CoV-2 virus is unprecedented, resistance against number of therapeutics and spreading rapidly with high mortality, which warrants the need to discover new effective drugs to combat this situation. This current study is undertaken to explore the antiviral potential of marine algal compounds to inhibit the viral entry and its multiplication using computational analysis. Among the proven drug discovery targets of SARS-CoV-2, spike glycoprotein and 3-chymotrypsin-like protease are responsible for the virus attachment and viral genome replication in the host cell. In this study, the above-mentioned drug targets were docked with marine algal compounds (sulfated polysaccharides, polysaccharide derivatives and polyphenols) using molecular docking tools (AutoDockTools). The obtained results indicate that κ-carrageenan, laminarin, eckol, trifucol and β-D-galactose are the top-ranking compounds showing better docking scores with SARS-CoV-2 targets, than the current experimental COVID-19 antiviral drugs like dexamethasone, remdesivir, favipiravir and MIV-150. Further, molecular dynamic simulation, ADMET and density functional theory calculations were evaluated to substantiate the findings. To the best of our knowledge, this is the first report on *in silico* analysis of aforesaid algal metabolites against SARS-CoV-2 targets. This study concludes that these metabolites can be curative for COVID-19 in the hour of need after further validations in *in vitro* and *in vivo* testings.

1. Introduction

The occurrence of viral outbreaks poses a severe threat to public health and economic loss in the present decade. In the last twenty years, viral epidemics such as SARS (severe acute respiratory syndrome) in 2002–2003, H1N1 influenza in 2009 and MERS (Middle East respiratory syndrome) in 2012 have been recorded (Cascella et al., 2021). SARS became a global epidemic that affected more than 8000 people from 30 countries, with a mortality rate of 9.2% (WHO, 2015), while MERS had been diagnosed with 2494 cases and caused 858 deaths, the majority are from Middle East countries especially Saudi Arabia. Both of these infectious diseases of humans were etiologically connected with coronaviruses (Drosten et al., 2003; Fouchier et al., 2003; Ksiazek et al., 2003; Marra et al., 2003; Peiris et al., 2003; Rota et al., 2003) and are listed in the priority list of pathogens (WHO, 2020b). In late December 2019, an outbreak of respiratory illness

with an unknown etiology happened in Wuhan, China, which was later diagnosed to be caused by a novel variant of coronavirus named 2019-nCoV/SARS-CoV-2 causing COVID-19 (Coronavirus infectious disease 2019) pandemic (Chen et al., 2020; WHO, 2020a). The SARS-CoV-2 virus primarily spreads through aerosols of saliva or nasal discharges of infected persons when coughed or sneezed, and recent evidence also showed the possibility of spread by airborne transmission. Coronaviruses belong to a family of single-stranded RNA (+ssRNA) viruses, found in various animal species (Perlman & Netland, 2009), which have crown-like structure or spikes made of glycoproteins, protrudes from its envelope. SARS-CoV-2 is the biggest known RNA virus comprises a genome size of 30 kb long (Chan et al., 2013). These spike proteins (S1 and S2 subunit) are essential to attach with the host cell receptor (ACE2) and assist virus entry inside the attached cells (International Pharmaceutical Federation, 2020; Weiss &

Navas-Martin, 2005). As of 18th November 2020, there have been over 5,52,43,538 cases, with 13,30,930 deaths from 216 countries for the pandemic outbreak of 2019-nCoV/SARS-CoV-2 worldwide. Besides, India has crossed 88,99,163 COVID-19 cases with 131,449 deaths.

The rapid spread of SARS-CoV-2 infections is a severe global public health threat, which has gained enormous attention globally for developing medications or therapeutic strategies to curb this unprecedented pandemic disease. Despite the expeditious collaborative and extensive research efforts from the research communities across the globe, there is still no approved medication or vaccine available yet to combat this deadliest disease. Thus, there is an urgent need to find novel therapeutics or repurposing the already existing antiviral drugs to combat the SARS-CoV-2 transmission to prevent pandemics. Moreover, SARS-CoV-2 has been classified into two major lineages based on genome sequences – 'L' and 'S' types, wherein 'L-type' has been evolved from 'S-type' and appears to be aggressive, highly infectious and contagious (Tang et al., 2020). Therefore, it is highly mandatory to provide adequate protection to people to reduce the high morbidity rate globally by finding novel drugs or vaccines. The genome of SARS-CoV-2 encodes various structural proteins, including envelop (E) protein, spike (S) protein (trimeric), nucleocapsid (N) and membrane (M) proteins. Spikes proteins are one of the crucial target sites because they help viruses attach to the target cells. Spike proteins are clove-shaped, type 1-transmembrane (TM) proteins and join together in a trimeric form on the outer membrane, appearing crown-like structure and play an essential role in entering host cells. Besides the viral genome encodes a replicase complex consisting of two polyproteins PP1a and PP1b, which are processed into 16 non-structural proteins by proteases including 3CL[Pro] (3-chymotrypsin-like cysteine protease) and PL[pro] (papain-like protease) that cleaves at C-termini and N-termini of the polyproteins, respectively (Kirchdoerfer & Ward, 2019). 3CL[Pro] is the crucial enzyme in viral replication and infection. Hence, spike glycoprotein and 3CL[Pro] have been considered as the prime targets for the treatment of SARS-CoV-2 infections. Subsequently, previously reported several inhibitors reported were repurposed against these targets, and most of them were failed to control viral infections effectively.

On the other hand, bioactive metabolites of natural origin are best suited and most consistently constructive sources for drug leads, especially products from marine sources as therapeutics are abundant. Several studies have been reported for marine antiviral drugs against HIV-1 (Human immunodeficiency virus type-1), HSV (Human herpes simplex virus), HBV (Hepatitis B virus), HCMV (Human cytomegalovirus), NoV (norovirus), RSV (respiratory syncytial virus) (Mayer et al., 2013). Marine algae are precious natural resources that are abundant with bioactive metabolites having potential therapeutic applications, which have not been much exploited. Algal secondary metabolites in particular polysaccharides, polyphenols, terpenes, acetogenins, phlorotannins and galactans have gained much attention recently due to their extensive biological potentials. Hence, there is

an excellent opportunity to discover metabolites of possible use for COVID-19. Thus, the present study explores the antiviral potential of polysaccharides, sulfated polysaccharides, sulfolipids and polyphenols from marine algae to target the SARS-CoV-2.

The conventional process of drug discovery is challenging, strenuous, costly, long and tedious. To overcome these challenges, computational tools like molecular docking has played a crucial role in rationalizing the path to drug discovery. A molecular docking methodology is currently a useful drug discovery tool that facilitates the rapid screening of candidates from drug libraries. Additionally, computational modeling of quantum chemical reaction, optimum structure and frontier molecular orbitals using density functional theory calculations are important to evaluate the molecular electrostatic potential, polarizability, dipole moment and thermal parameters of the drugs. Further, the molecular docking studies are generally validated using Molecular Dynamic simulation that evaluates the structural stability, interactions and constancy of macromolecule interactions with the ligand. The *in silico* ADMET profiling is widely applied in the drug-discovery process for predicting the absorption, distribution, metabolism and excretion of drug molecules which plays an important role in the screening of drugs for clinical phases.

Therefore, this investigation is mainly aimed to develop effective therapeutics using polysaccharides, sulfated polysaccharides and polyphenols to inhibit the two main protein targets of SARS-CoV-2 by molecular docking studies. Further, the efficiency of all the algal ligands interaction with the viral targets was also compared with the commercial antiviral drugs currently used against the COVID-19 pandemic.

2. Methods and computational details

2.1. Target sites

To explore the suitable antiviral agents against SARS-CoV-2/nCoV2, twenty-two algal compounds were chosen as ligands to interact with the two main targets (Spike glycoprotein & 3CL protease) of SARS-CoV-2. The two target proteins, Main protease(M[pro])/3-Chymotripsin-like protease (3CL[pro]) (PDB ID 6Y2E (Zhang et al., 2020)) and spike glycoprotein (PDB ID 6VYB (Walls et al., 2020)) crystal structures were downloaded from the Protein Data Bank (PDB) and HETATM (hetero atom, non-stranded residues) were removed. This spike glycoprotein has three heterotrimer polypeptide chains A chain, B chain and C chain. Among these three chains, C chain is used as the target from spike glycoprotein for the molecular docking studies. The C chain was separated from the heterotrimer chain by the Discovery Studio 2020 (Dassault System BIOVIA) visualization tool and saved as PDB format for further docking studies.

2.2. Ligand preparation

The marine algal bioactive compounds such as polysaccharides, sulfated polysaccharides (SPs), polyphenols,

polysaccharide derivatives and sulfolipid were chosen as ligands for the target proteins. The ligands structures were retrieved from the PubChem database (Kim et al., 2019) in the form of 3D structure data file (SDF), the 3D structure of the ligands with 2D SDF format were derived from the Discovery Studio 2020 visualization tool and PyMol visualization tool (Schrödinger, Inc.) (DeLano, 2014). Similarly, four commercially available experimental drugs against SARS-CoV-2, such as dexamethasone, remdesivir, favipiravir and MIV-150 were also docked with the 3CL protease and spike glycoprotein as a positive control for the comparative analysis of the docking studies. The structure of the aforesaid four drugs was retrieved from the PubChem databases in the SDF format and, 3D structures were built in PyMol viewer. The collectively retrieved 3D structures in the format of PDB were further used for the docking studies. The 2D structures of all ligands are listed in Supplementary Figure 1.

2.3. Molecular docking

Molecular docking studies were carried out using AutoDockTools (ADT) (Scripps Research US) (Morris et al., 2009) with the extension suite to the Python Molecular Viewer of MGL tools with Cygwin program (Rizvi et al., 2013). Protein and ligand preparations were carried out in ADT. The preparation of target protein was initiated by the deletion of water, addition of polar hydrogen and merging of nonpolar hydrogen. Later the Gasteiger and Kollman charges were added to ligand and protein before the preparation of the grid parameter file, respectively.

The docking studies were performed using the Lamarckian genetic algorithm (LMA) and empirical free energy function with a standard protocol (Forli et al., 2016; Rizvi et al., 2013). The parameters of the Genetic Algorithm comprise a maximum number of 2.5×10^6 energy appraisals, a maximum number of 2.7×10^4 generations and a rate of mutation 0.02 with 0.8 crossover rate. Pseudo Solis & Wets parameters for local search (LS) were performed, and 300 iterations of Solis & Wets for the local search were introduced. Totally, 50 independent runs were assigned for each compound using ADT. All the structures produced from the lowest-energy structure were assigned to clusters after docking based on a tolerance of 2 Å Root Mean Square Deviation (RMSD). AutoDock program detects appropriate dockings in a protein-binding site, using LMA by starting with a ligand in an arbitrary conformation, position and orientation. Among the 50th run, the ideal docking result was examined by the conformation with the lowest binding energy and lowest RMSD value in ADT. The protein and ligand interactions were analyzed with the hydrogen bonding, hydrophobic interactions, 2D structure interaction in the Discovery Studio tool (Biovia, 2016).

2.4. Molecular dynamics simulation

Molecular Dynamics (MD) simulation for interaction analysis of SARS-CoV-2 main protease with selected compounds were performed using Desmond tool of Schrödinger Maestro platform (Schrödinger Release, 2019). Based on the molecular interaction and docking scores, the top-ranked compounds were selected for the Molecular Dynamics (MD) simulation analysis. The macromolecule and ligand complex was solvated using the three-dimensional orthorhombic box with a buffer distance of 10 Å and 853903 Å³, respectively, to build a hydration model (TIP3P water model) using System builder tool in Desmond. The water-filled box system was neutralized with counter-ions, and the addition of 150 mM of NaCl ions to mimic physiological conditions. The system energy was minimized and the macromolecule-ligand complex system was designated with the OPLS3 force field.

Next, the MD simulations were set up for 200 ns under NPT ensemble (constant number of atoms (N), constant pressure (P) and temperature (T)) where the model system was relaxed prior to simulation using the default Desmond settings. Subsequently, the MD simulations were analyzed graphically by applying a simulation interactive diagram tool that provided data on complex macromolecule-ligand properties during the simulation phase. To further substantiate the molecular docking results, RMSF (root mean square fluctuation), RMSD (root mean square distance) and bond interaction data were interpreted.

2.5. Density functional theory (DFT) calculations

The optimum geometric structure of the ligands without imaginary frequency were developed by energy minimization and the virtual image were portrayed using Gauss view 5, Gaussian 09 software (Gaussian 09, n.d.), the basic set for the DFT calculation was carried out by B3LYP 6–311 G (d, p). The ground state-HOMO (Highest Occupied Molecule Orbital) and excitation state-LUMO (Lowest Un-occupied Molecular Orbital) of the drug were expressed in electron volt (Hartree atomic units). The energy difference between the HOMO and LUMO were measured, concurrently the electrophilicity, electronegativity, global hardness and global softness were determined by the following equation (Hagar et al., 2020)

$$Global\ hardness\ (\eta) = [-1/2\ (E_{HOMO} - E_{LUMO})] \quad (1)$$

$$Global\ softness\ (\delta) = [1/\eta] \quad (2)$$

$$Electronegativity\ (\chi) = [-1/2\ (E_{HOMO} + E_{LUMO})] \quad (3)$$

$$Electrophilicity\ (\omega) = \chi^2/2\eta \quad (4)$$

2.6. In silico pharmacokinetic and toxicological properties using ADMET profiling

The *in silico* pharmacokinetics and pharmacodynamics evaluation of top-ranked marine algal compounds were evaluated for drug-likeness by computational ADMET profiling (Adsorption, distribution, metabolism, excretion and toxicity) using Qikprop module in Schrodinger's Maestro platform. The physicochemical descriptors were compared with the reference values of the QikProp 3.5 User Manual to predict the pharmaceutically relevant properties of the compounds (QikProp, version 3.5., Schrödinger).
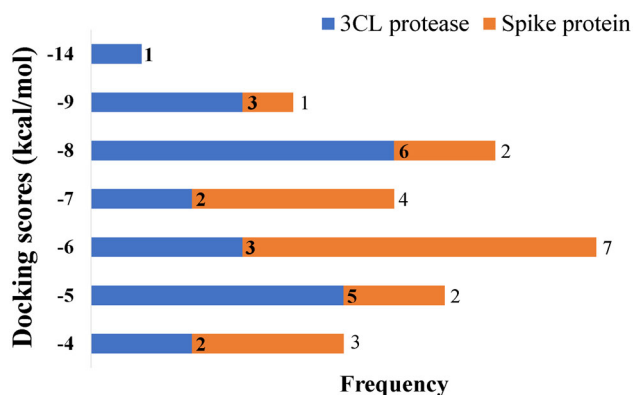
Figure 1. Frequency distribution of 22 potent marine algal compounds over the range of docking scores with SARS-CoV-2 target proteins 3CL^{Pro} and spike glycoprotein.

3. Results and discussion

A total of 22 naturally occurring compounds of marine algal origin consisting of non-sulfated polysaccharides, polyphenols, sulfated polysaccharides and their derivatives with the potential of antiviral, anti-microbial, anti-oxidant, anti-inflammatory and immunomodulatory activities were investigated herein for their inhibitory effects against SARS-CoV-2 targets such as spike protein and 3CL^{pro} by molecular docking analysis. In addition, dexamethasone, remdesivir, favipiravir and MIV-150, the known antiviral drugs currently used as experimental anti-COVID-19 drugs were used as positive controls. Binding scores of the marine algal compounds are distributed within the range of −1.0 to −4.0, −4.1 to −5.0, −5.1 to −6.0, −6.1 to −7.0, −7.1 to −8.0, −8.1 to −9.0 and −14.0 to −15.0 kcal/mol (Figure 1).

3.1. Molecular interaction of marine algal ligands and targets of SARS-CoV-2

3.1.1. Sulfated polysaccharides

Sulfated polysaccharides are heterogeneous natural polymers found abundant in marine algae, which exert a different range of pharmacological applications due to the large variability in its chemical structure and composition (Wang et al., 2018). Sulfated polysaccharides of marine algal origin like carrageenan and fucoidan have been shown to exert antiviral activities by controlling the viral replication via blocking the binding of virions with their target cells (Baba et al., 1990). In this study, some of the selected sulfated polysaccharides with antiviral potentials were evaluated for their binding affinity with the target proteins of SARS-CoV-2 (Figures 2–4).

Besides, the fucoidan forms the inhibitory complex with the proteins of the human hepatocellular carcinoma (HepG2) cell line and the docking score were maximum for Caspase-3 (−12.30 kcal/mol) having one hydrogen bond, NF-kappa-B (−11.57 kcal/mol) with three hydrogen bond and Cytochrome C (−9.88 kcal/mol) with one hydrogen bond (Jayameena et al., 2018). In addition, the antiviral activity of fucoidan toward Newcastle disease virus (NDV) has been reported (Elizondo-Gonzalez et al., 2012). Similarly,

carrageenan found to have a broad range of antiviral activity against herpes simplex virus, dengue virus, papillomavirus, hepatitis A virus, rhinovirus, herpes simplex virus and various enveloped viruses as influenza A virus, human immunodeficiency virus, cytomegalovirus, vesicular stomatitis virus, porcine reproductive and respiratory syndrome virus (Eccles, 2020). Another potent sulfated compound, sulfoquinovosyl diacylglycerol (SQDG) are a class of sulfolipids containing glycolipids with sulfur, found in algae and other photosynthetic organisms. SQDG isolated from various algal species exhibits potent antiviral activity, particularly against HIV-1 with cytopathic effect inhibition, HSV-2 (selectively inhibiting replication), antitumor-promoting properties and moderate antiviral against HSV-1 and Coxsackievirus B3 (Cox B3) (De Souza et al., 2012; Gustafson et al., 1989; Plouguerné et al., 2013; Shirahashi et al., 1993). SQDG from red alga *Gigartina tenella* primarily acted on HIV-1 by inhibiting DNA polymerase α and β and HIV-RT (HIV-reverse transcriptase type 1) (Ohta et al., 1998).

These findings of *in silico* studies are strong evidence for the potential antiviral properties of these sulfated polysaccharides against SARS-CoV-2 because of their promising interaction with spike glycoprotein and 3CL^{pro}. Moreover, it is noteworthy to mention that the presence of polysulfates on sulfated polysaccharides results in a highly negative charge that would facilitate the interaction with viral spike glycoproteins due to the presence of positively charged ions on its surface (Damonte et al., 2012). Sulfated polysaccharides against HIV and HSV have been widely used, but it is not yet tested against SARS-CoV-2. Also, sulfated polysaccharides are attracting molecules that can able induce diverse immune cells and also have the ability to act as an adjuvant for treating immunological disorders (Bi et al., 2018; Mei et al., 2017). Furthermore, sulfated polysaccharides from various natural resources had exerted intense immunomodulatory activity by inducing the macrophages to secrete the cytokines (Barbosa et al., 2019), which is highly essential to maintain the secretion of cytokines in SARS-CoV-2 infected individuals.

The present study revealed a noticeable interaction of alpha-carrageen, carrageen-lambda and 3,6-anhydro-D-galactose-2-sulfate with the spike glycoprotein were observed (Figure 5). Among the twenty-two ligands, the κ-carrageenan had shown the best highest binding energy (−14.37 kcal/mol) and lower inhibition constant (Ki = 29.35 pM) (Table 1a,b) with 3CL^{pro} interaction compared to the commercial antiviral drugs dexamethasone, remdesivir, favipiravir and MIV-150. Likewise, ß-carrageenan showed higher binding affinity with 3CL^{pro} compared to remdesivir and favipiravir. Additionally, κ-carrageenan, carrageenan-lambda, ß-carrageenan, sulfoquinovosyl diacylglycerol and fucoidan showed even better docking scores with spike glycoprotein compared to that of all positive controls (antiviral drugs). Thus κ-carrageenan, ß-carrageenan and carrageenan-lambda may be used as an antiviral drugs to prevent the multiplication of the virus in the host cells, once after conducting the preclinical studies to validate its potential further.
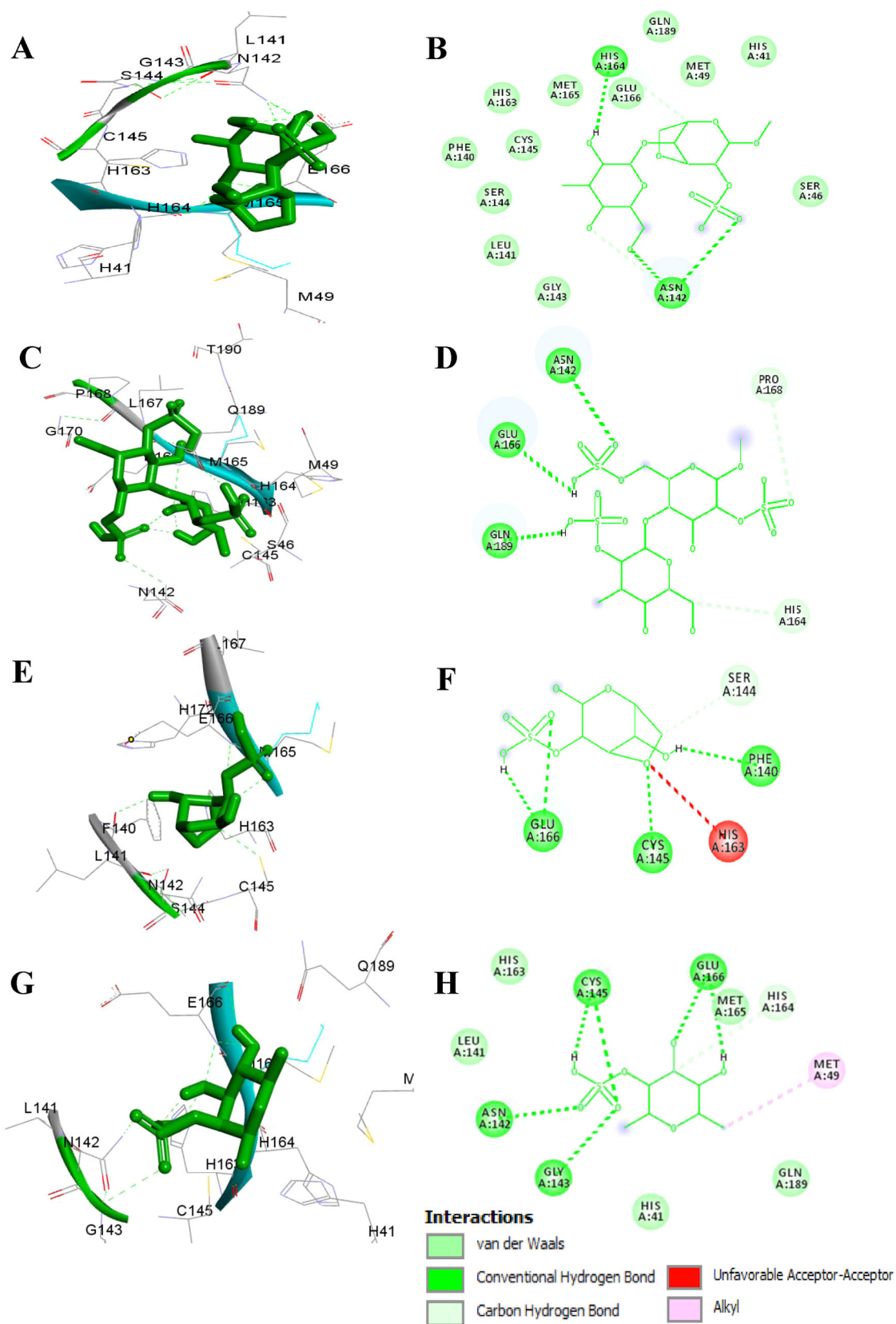
Figure 2. Molecular interaction of marine algal sulfated polysaccharides with 3CL^{Pro} of SARS-CoV-2. (A & B) The interaction of α-carrageenan with 3CL^{Pro} and their respective 2D structure; (C & D) The interaction of λ-carrageenan with 3CL^{Pro} and their respective 2D structure; (E & F) The interaction of 3,6-anhydro-D-galactose-2-sulfate with 3CL^{Pro} and their respective 2D structure; (G & H) The interaction of fucoidan with 3CL^{Pro} and their respective 2D structure.

3.1.2. Non-sulfated polysaccharides

In the recent scenario, many investigations are being carried out to exploit the marine algae as the richest source of

bioactive metabolites for treating communicable and non-communicable diseases. Polysaccharides abundantly synthesized from algae are considered non-toxic, cheap, safe,
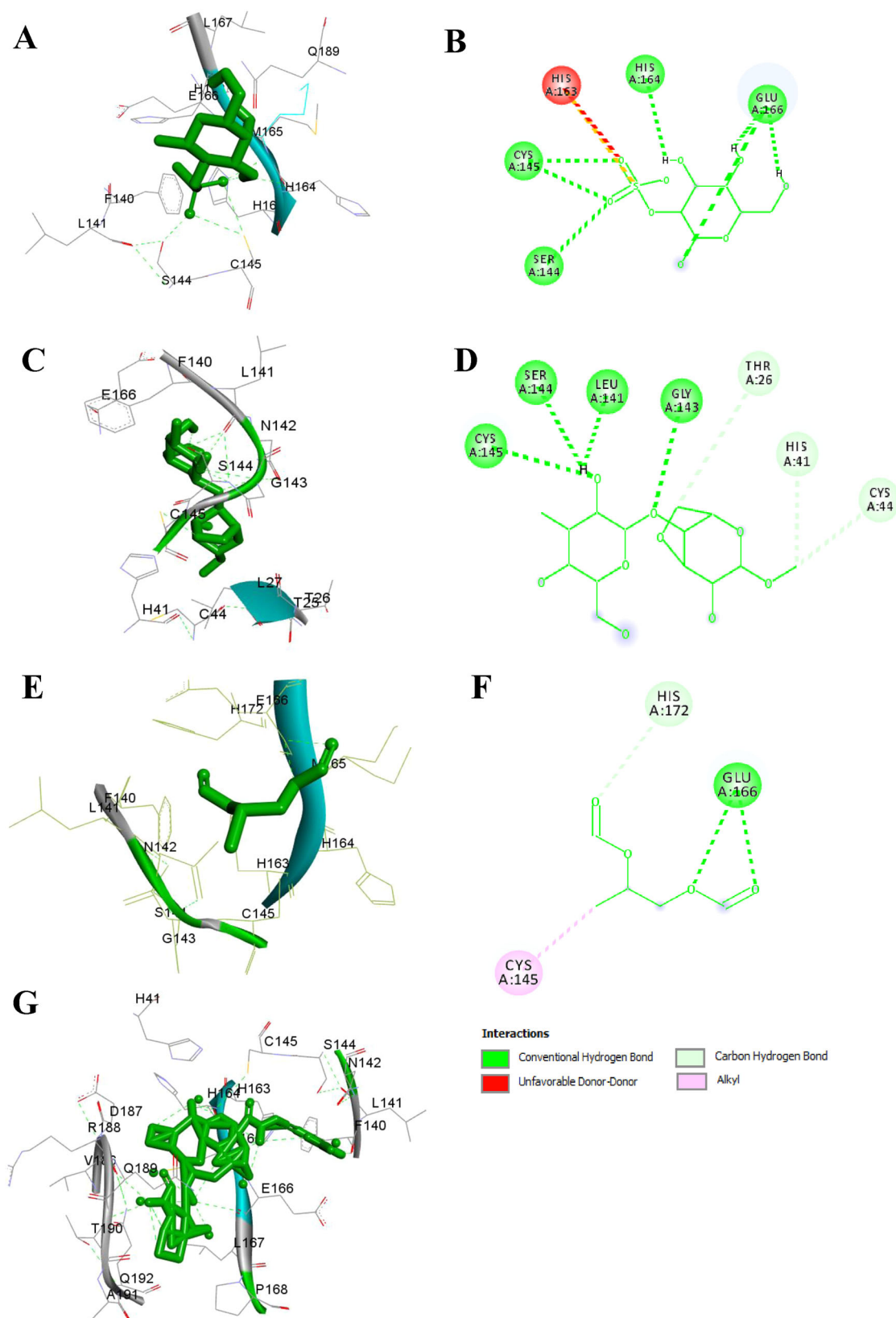
Figure 3. Molecular interaction of marine algal sulfated polysaccharides with 3CL^{Pro} of SARS-CoV-2. (A & B) The interaction of carrageenan-lambda with 3CL^{Pro} and their respective 2D structure; (C & D) The interaction of β-carrageenan with 3CL^{Pro} and their respective 2D structure; (E & F) The interaction of sulfoquinovosyl diacylglycerol with 3CL^{Pro} and their respective 2D structure; (G) The interaction of κ-carrageenan with 3CL^{Pro}.
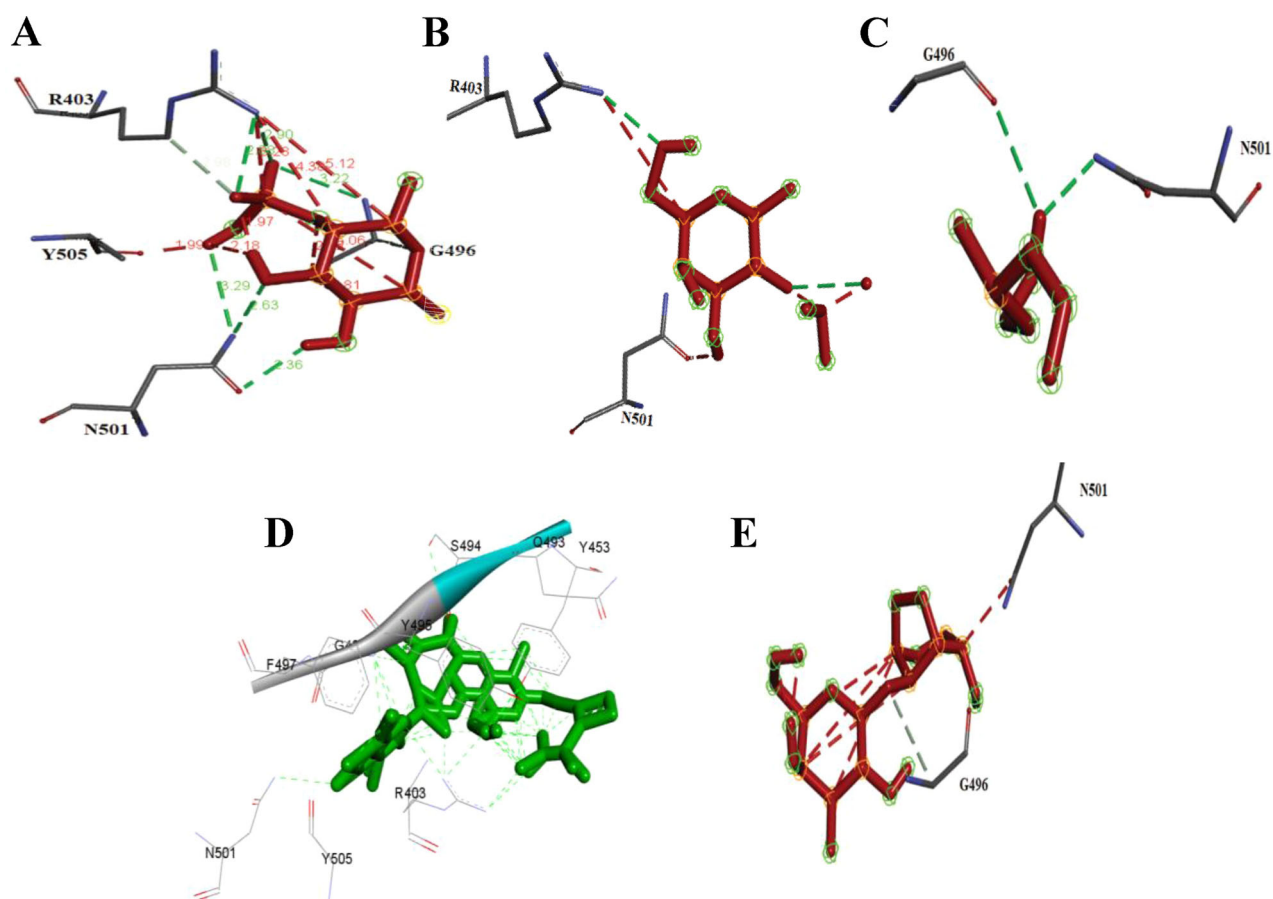
Figure 4. Molecular interaction of marine algal sulfated polysaccharides with spike glycoprotein of SARS-CoV-2. (A) Fucoidan; (B) Carrageenan-lambda; (C) Sulfoquinovosyl diacylglycerol; (D) κ-carrageenan; (E) β-carrageenan.
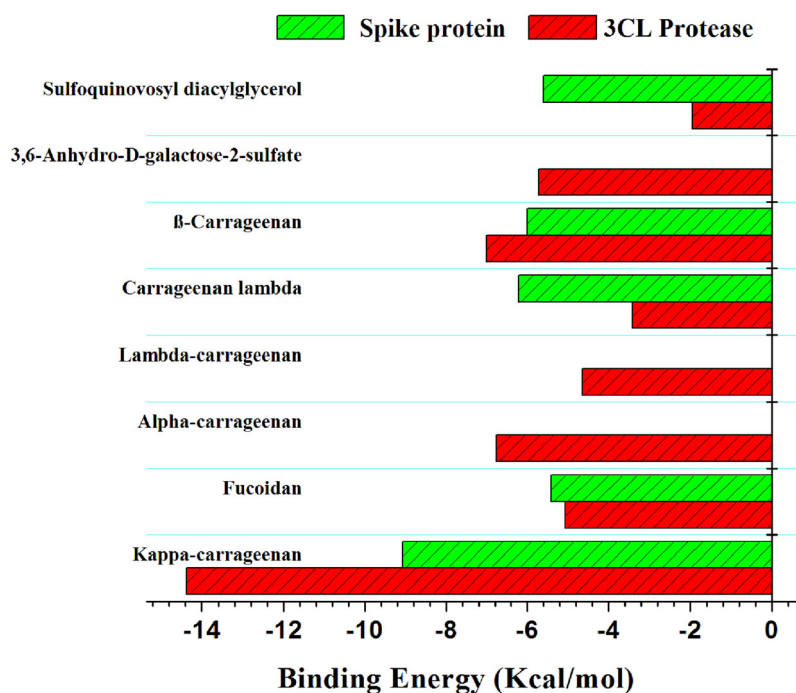
Figure 5. Comparison of the binding affinity of sulfated polysaccharides with spike glycoprotein and 3CL[pro] of SARS-CoV-2.

Table 1a. Binding interaction parameters of marine algal sulfated polysaccharides with 3CL^{pro} protein target of SARS-CoV-2, where, Ki = inhibition constant and H = hydrogen bond.

Compound name	PubChem CID	3CL Protease				
		Binding energy (kcal/mol)	Ki	Interactive residue	Bond type	Bond length (Å)
κ-carrageenan	11966249	−14.37	29.35 pM	F140	H	3.00
				H164	H	2.50
				E166	H	2.85
				Q192	H	3.92
				T190	H	2.85
α-carrageenan	102199625	−6.77	10.87 μM	H164	2H	2.60, 3.51
				N142	3H	2.73, 2.81, 2.88
λ-carrageenan	101231953	−4.65	393.13 μM	N142	H	3.12
				E166	H	2.59
				H164	H	3.60
				P168	H	3.13
				Q189	H	1.76
3,6-anhydro-D-galactose-2-sulfate	446806	−5.42	105.91 μM	F140	H	2.20
				S144	H	2.86
				C145	H	2.75
				H163	H	3.00
				E166	2H	1.75, 2.68
Fucoidan	92023653	−5.08	188.66 μM	N142	H	2.92
				G143	H	3.10
				C145	H	2.68
				E166	H	2.78
Carrageenan-lambda	91972149	−3.42	3.12 mM	S144	H	3.04
				C145	2H	3.10, 3.08
				H163	2H	2.81, 4.27
				H164	H	2.49
				E166	4H	1.80, 2.05, 3.27, 2.48
ß-carrageenan	102199626	−7.01	7.21 μM	T26	H	3.78
				H41	H	3.04
				C44	H	3.02
				L141	H	1.74
				S144	H	2.35
				C145	2H	3.25, 3.30
Sulfoquinovosyl diaceylglycerol	SID 586228	−1.95	37.11 mM	C145	H	3.93
				H172	H	3.34
				E16	2H	2.86, 2.97

Table 1b. Binding interaction parameters of marine algal sulfated polysaccharides with spike glycoprotein target of SARS-CoV-2, where, Ki = inhibition constant and H = hydrogen bond.

Compound name	PubChem CID	Spike glycoprotein				
		Binding energy (kcal/mol)	Ki	Interactive residue	Bond type	Bond length (Å)
κ-carrageenan	11966249	−9.07	225.55 nM	Y453	2H	2.58, 2.85
				G496	2H	2.85, 2.93
				R403	5H	2.71, 2.76, 3.00, 3.18, 3.21
				N501	H	3.07
α-carrageenan	102199625		Weak interaction			
λ-carrageenan	101231953		Weak interaction			
3,6-anhydro-D-galactose-2-sulfate	446806		Weak interaction			
Fucoidan	92023653	−5.42	105.57 μM	R403	2H	2.88, 2.90
				N501	3H	2.36, 2.62, 3.29
				G496	H	3.22
Carrageenan-lambda	91972149	−6.22	27.66 μM	R403	H	2.62
				N501	H	2.04
ß-carrageenan	102199626	−6	39.78 μM	G495	H	2.77
				N501	H	3.71
Sulfoquinovosyl diaceylglycerol	SID 586228	−5.61	77.79 μM	G496	H	3.25
				N501	H	2.71

biocompatible and biodegradable (Ahmadi et al., 2015). Also, these polysaccharides are being commercially produced in pharmaceutical industries for its wider applications. In this context, some of the potential non-sulfated polysaccharides structures exclusively from algae were retrieved from the PubChem database and have been used for molecular docking studies with the selected targets of SARS-CoV-2. Interestingly, the docked results attained from AutoDockTools had revealed that the top-ranking ligand was laminarin based on the highest binding energy, lower Ki and highest hydrogen bonds with both spike glycoprotein and 3CL^{pro} of SARS-CoV-2 (Table 2a,b).

Laminarin is found in brown algae, which is a storage glucan of linear polysaccharide consisted of β-1,3 linkage with glucose and β-1,6 linkage in side-chain branching. Laminarin is exploited for several antiviral potentials against HIV, works

Table 2a. Binding interaction parameters of marine algal non-sulfated polysaccharides with 3CL^{Pro} protein target of SARS-CoV-2, where, Ki = inhibition constant, H = hydrogen bond & nH = non-hydrogen bond.

Compound name	PubChem CID	3CL Protease				
		Binding energy (kcal/mol)	Ki	Interactive residue	Bond type	Bond length (Å)
Alginate	91666318	−4.76	323.05 μM	F140	H	2.19
				L141	H	1.90
				S144	H	2.86
				C145	H	3.56
				E166	H & nH	2.76, 2.65
Laminarin	439306	−7.81	1.89 μM	T190	nH	3.71
				E166	H & nH	1.97, 2.65
				Q189	2H & nH	2.41, 2.25, 3.02
β-Glucan	53477780	−7.30	4.44 μM	H164	2H	2.17 & 2.02
				E166	3H	3.27 & 2.77
				P168	H	2.02
				Q189	2H	1.76 & 2.58

Table 2b. Binding interaction parameters of marine algal non-sulfated polysaccharides with spike glycoprotein target of SARS-CoV-2, where, Ki = inhibition constant and H = hydrogen bond.

Compound name	PubChem CID	Spike glycoprotein				
		Binding energy (kcal/mol)	Ki	Interactive residue	Bond type	Bond length (Å)
Alginate	91666318	−5.83	52.92 μM	R403	2H	2.91, 2.92
				Y453	H	2.74
				S494	3nH	1.85, 1.78, 2.15
				Y495	nH	2.74
Laminarin	439306	−7.83	1.82 μM	R403	H	2.56
				S494	2H & 2nH	3.25, 3.08, 2.02, 1.91
				G496	H & 2nH	3.32, 2.07, 2.11
				N501	H	2.68
β-Glucan	53477780	−4.91	252.94 μM	R403	nH	5.56
				S494	nH	2.08
				G496	H	3.18
				N501	H	2.38

by inhibiting the reverse transcriptase mechanism leading to non-proliferation of the virus. And this is the first to report to dock laminarin with SARS-CoV-2 3CL^{Pro}.

β-glucan also resulted in a strong binding affinity with 3CL^{Pro}. β-glucans are structural non-starch polysaccharides consisting of β-D-glucose monomer units holding by glycosidic linkages. β-glucans are obtained from brown algae cell walls such as *Laminaria* sp. and also extracted from bacteria, fungi and lichens. β-glucan has hypoglycemic, prebiotic, anticancer, antihypertensive, wound healing, immune-boosting, antiviral and antibacterial properties (Kaur et al., 2020; Raimundo et al., 2017). β-glucan from *Aspergillus brasiliensis* has been exploited for antiviral potential against bovine herpesvirus (BoHV-1) and the inhibition of viral replication has been demonstrated by plaque assay (Minari et al., 2011). Besides, β-glucans have multifunctional features, including host defense mechanisms, enhancing the immune response, T-cell activation, anti-inflammatory and also can bind to macrophages and other polymorphonuclear cells (Gantner et al., 2003; Herre et al., 2004; Kim et al., 2019). Moreover, it is well known that the immune functions such as secretion of cytokines (IL-1, IL-6 and GMCSF), phagocytosis, interferons and antigen processing are improved when the β-glucan receptor is occupied with β- 1,3/1,6 glucan (Meena et al., 2013). Previously, it has been reported that β-1,3-glucan interacts with the dectin-1 enzyme, which plays an important role in tumor cell-associated glycosylation. The tumor cells show excess production of dectin-1 and also stated that it plays a vital role in activating immunological responses by interacting with β-1-3 glucan. The Dectin-1 is a transmembrane protein (type II)

present on leukocytes surface, showed the highest levels of cell surface expression in macrophages, neutrophils and dendritic cells (Chiba et al., 2014). Similar effects of β-glucan on immunological response activation may be effective in immune-compromised patients with COVID-19.

Next to laminaran, β-glucan and alginate had shown a promising interaction with both spike glycoprotein and 3CL^{pro} (Figures 6–8). Alginates are comprised of poly-D-glucuronic acid and poly-D-mannuronic acid (Mabeau & Kloareg, 1987; Wang et al., 2012) that are present majorly in the brown algae *Laminaria japonica*, *Ascophyllum nodosum*, *Laminaria digitata* and *Laminaria hyperborean*. These are acidic polysaccharides comprise various biomedical applications especially used as an immune activator, and importantly the antiviral potential of alginate as 911 drug has also been reported against HIV as reverse transcriptase inhibitor and blocking the DNA polymerase activity in Hepatitis B virus (HBV) (Xianliang et al., 2000). Recently it has also been reported that by alginate supplemented therapy immune tolerance can be enhanced in COVID-19 patients (El-Sekaily et al., 2020).

Hence, the above-mentioned report of polysaccharides are exploited as antiviral drugs against the enveloped viruses, and these evidence are substantiated with the *in silico* analysis performed in this study for the aforesaid polysaccharides.

3.1.3. Derivatives of seaweed polysaccharides

Additionally, algal polysaccharides and sulfated polysaccharides were reported to have antiviral activity for various
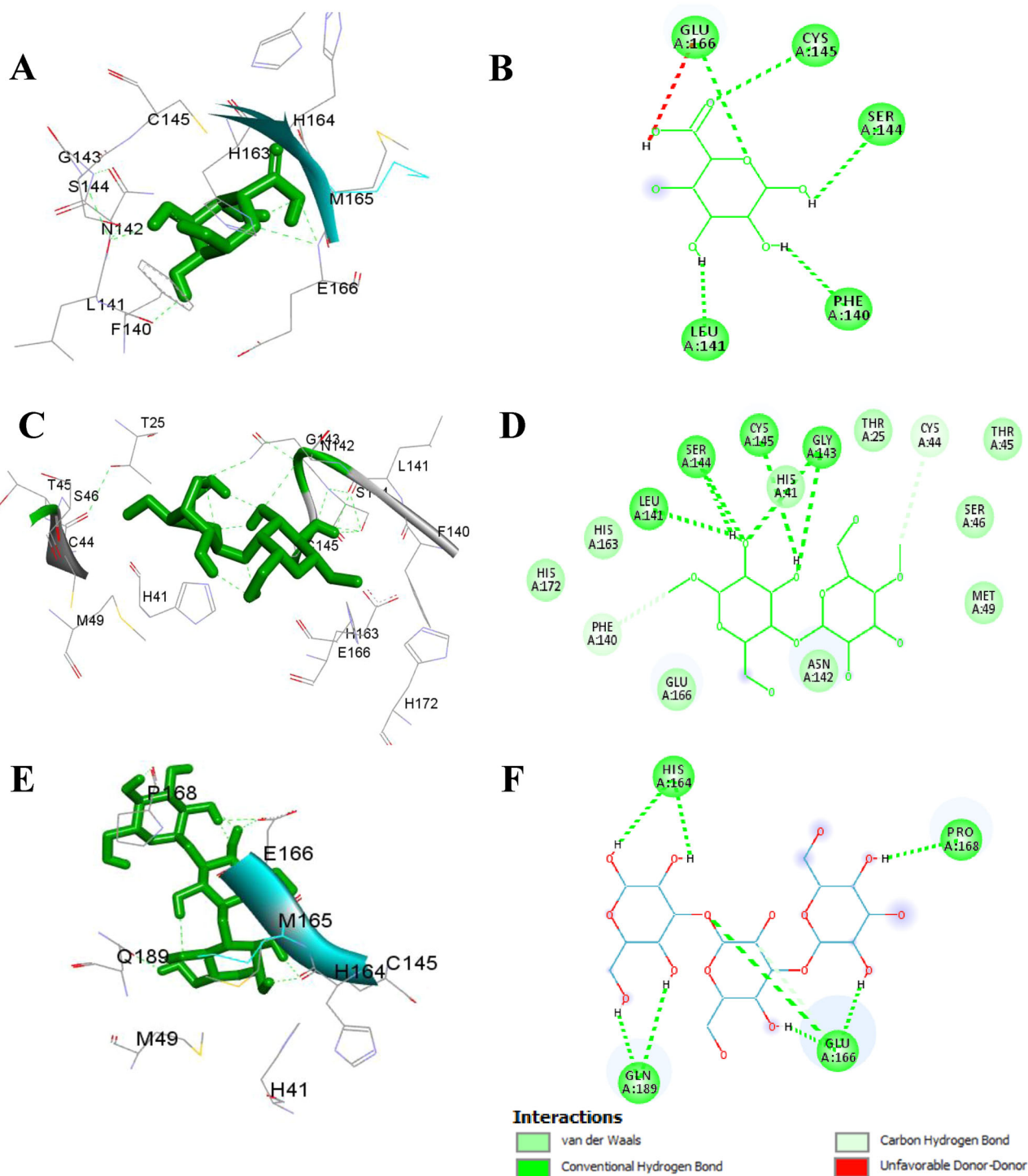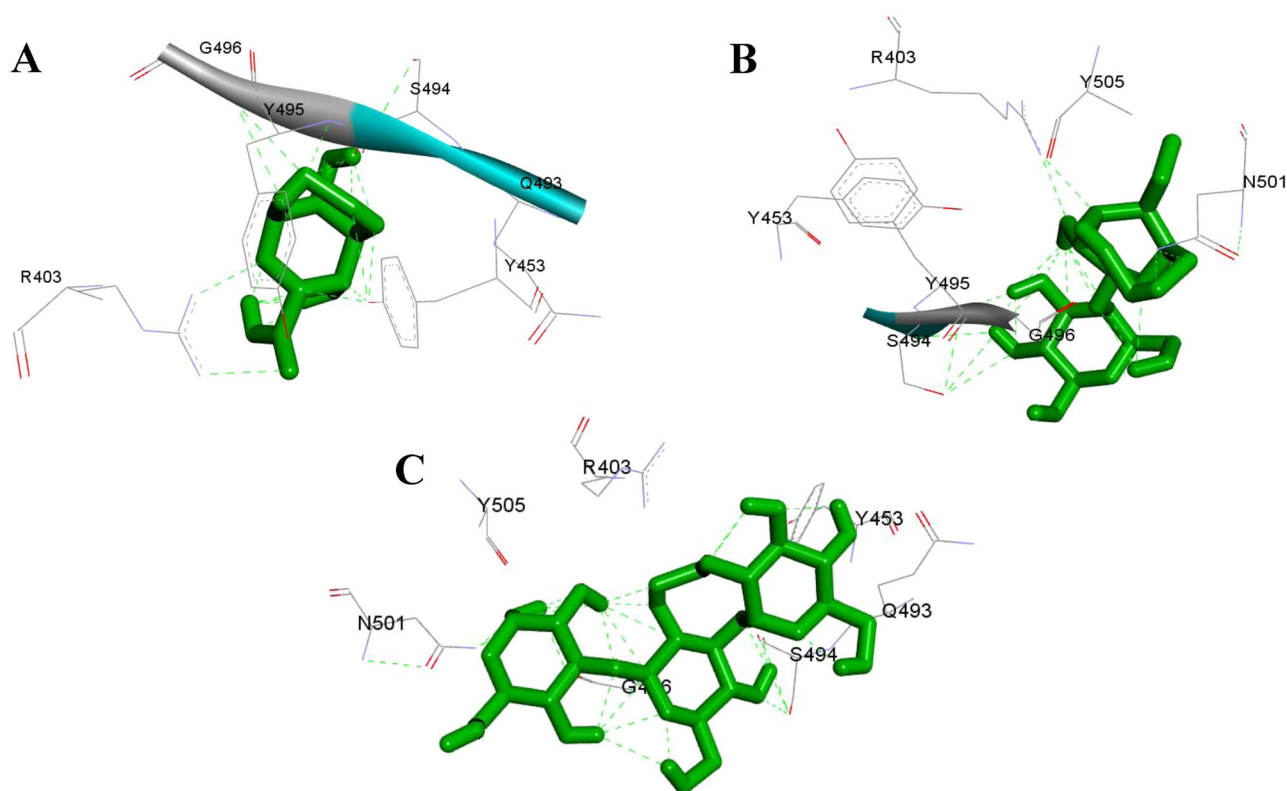
Figure 6. Molecular interaction of marine algal non-sulfated polysaccharides with 3CL^Pro of SARS-CoV-2. (A & B) The interaction of alginate with 3CL^Pro and their respective 2D structure; (C & D) The interaction of β-glucan with 3CL^Pro and their respective 2D structure; (E & F) The interaction of laminarin with 3CL^Pro and their respective 2D structure.

enveloped viruses herein the derivatives of sulfated polysaccharides were also included for *in silico* analysis. The carbohydrates and its derivatives are involved in various processes and pathways of marine organisms survival in the harsh marine environment. Some sulfated polysaccharide derivatives of red seaweed possess selective antiviral properties against HSV-1 and HSV-2 (Duarte et al., 2004). Moreover, red algae *Acanthophora spicifera* derivatives block the virus entry by interfering with the initial attachment of the virus to the target cell. However, the antimicrobials from the non-sulfated carbohydrates are scarce. Thus, this study would specifically emphasize the interaction with the derivatives of polysaccharides and sulfated polysaccharides from algae, which were retrieved from PubChem, examined by molecular docking and the comparative binding scores of ligands with the two targets of SARS-CoV-2 were depicted in Figures 9–12.

Interestingly all the ligands used in this docking experiment had shown the interaction with some specific amino

Figure 7. Molecular interaction of marine algal non-sulfated polysaccharides with spike glycoprotein of SARS-CoV-2. (A) Alginate; (B) β-glucan; (C) Laminarin.
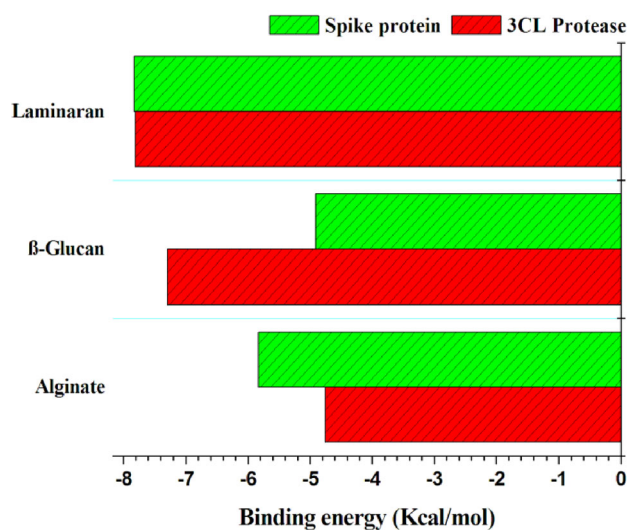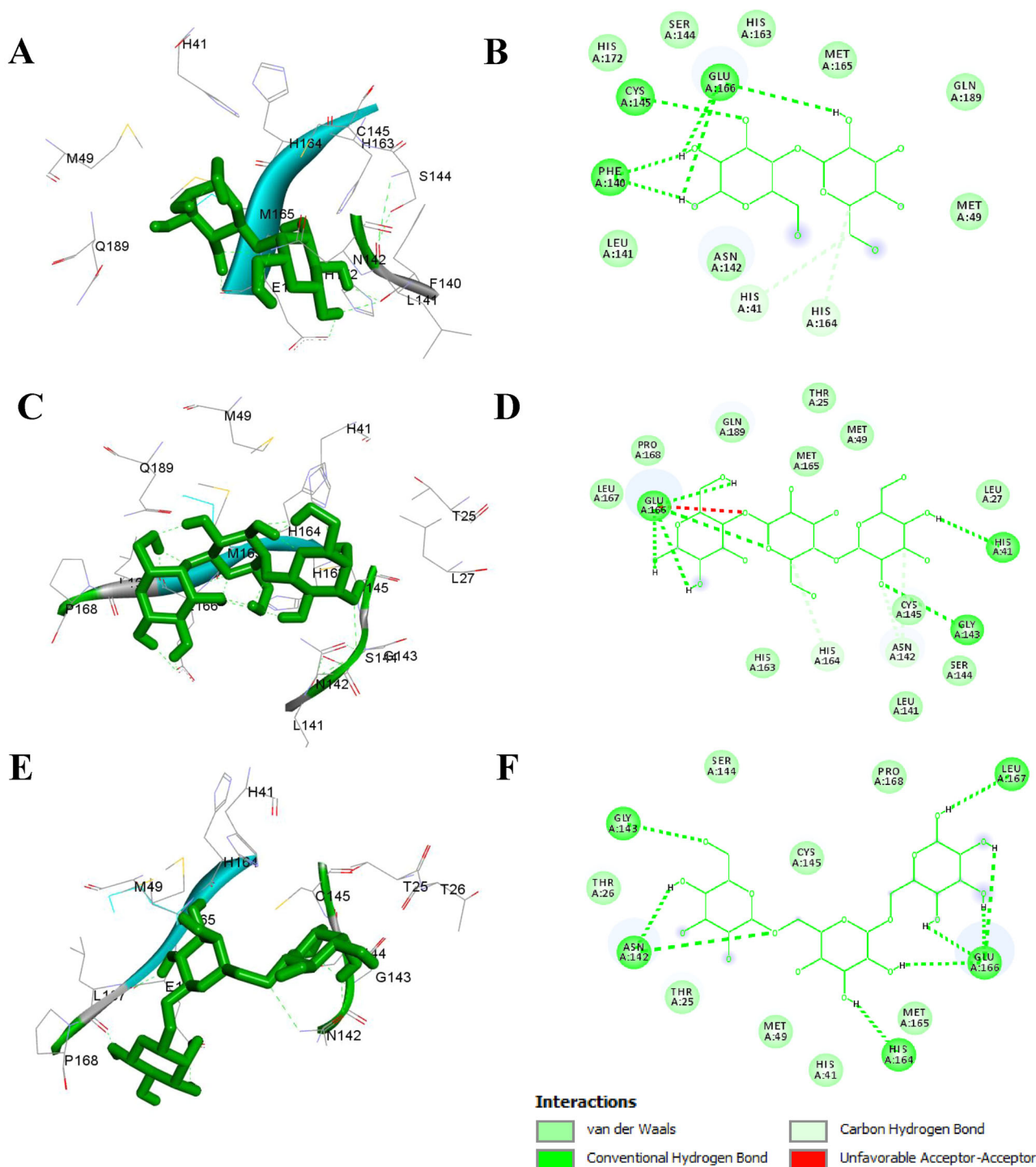

Figure 8. Comparison of the binding affinity of non-sulfated polysaccharides with SARS-CoV-2 targets (spike glycoprotein and 3CL^{pro}).

acid of the targets like Glu166, Gln189, Cys145, Phe140. In addition, almost all the derivatives of polysaccharides have shown the interaction with 3CL^{pro} and spike glycoprotein with high binding energy, low Ki and higher hydrogen bonds. It is noteworthy to mention that β-galactan ranks first when compared with all other derivatives of polysaccharides because of the higher binding energy with 3CL^{pro} and spike glycoprotein (−8.26 and −6.24 kcal/mol) followed by β-1,3-galactotriose, galactobiose, β-1,6-galactotriose and dialphaGal, which also showed best binding energy and Ki with both the targets (Table 3a,b).

The chemical description of the compounds is as follows: β-1,6-galactotriose and β-1,3-galactotriose belongs to the class of organic compounds known as oligosaccharides. β-1,3-galactotriose is a derivative of lambda-carrageenan; a trisaccharide composed of three β-D-galactose units joined by (1→3)-linkages whereas, β-1,6-galactotriose are joined by (1→6)-linkages (Lawson & Rees, 1968). Galactobiose is also called as β-D-galactopyranosyl-1,4-β-D-galactopyranose, and these are derivatives of κ-carrageenan (O°Neill, 1955). Galactotriose is a trisaccharide consists of three hexose carbohydrate units linked to each other through glycosidic bonds, it is also a type of laminarin which serves as a storage glucan in brown algae (Dictionary of Food Compounds with CD-ROM, 2013). β-galactan is a polysaccharide consisting of polymerized galactose residues joined by β-(1→4)-glycosidic linkages found in red seaweeds (Delattre et al., 2011). 3,6-anhydro-D-galactose is a constituent of a sulfated polysaccharide κ-carrageenan obtained from red macroalgae. This κ-carrageenan consists of an alternating backbone of D-galactose-4-sulfate and 3,6-anhydro-D-galactose (Kim & Lee, 2016). DialphaGal is a glycosylgalactose that constitutes two units of D-galactose linked by α-(1→3) linkage, which can act as an epitope or antigen. This is also intrinsic to the chemical structure of carrageenan. It is also primarily found in mammals excluding humans; it's derivative α-Gal epitope that is considered as a vaccine candidate for HIV infection since it can induce antibodies in the system. It has been reported that α-Gal induced antibodies can enhance immunogenicity in HIV vaccination (Abdel-Motal et al., 2010), assist in curing burn injuries (Galili et al., 2010),

Figure 9. Molecular interaction of marine algal polysaccharides derivatives with 3CL^Pro of SARS-CoV-2. (A & B) The interaction of 3,6-anhydro-D-galactose with 3CL^Pro and their respective 2D structure; (C & D) The interaction of β-(1-3)-galactotriose with 3CL^Pro and their respective 2D structure; (E & F) The interaction of dialphaGal with 3CL^Pro and their respective 2D structure; (G & H) The interaction of β-galactan with 3CL^Pro and their respective 2D structure.
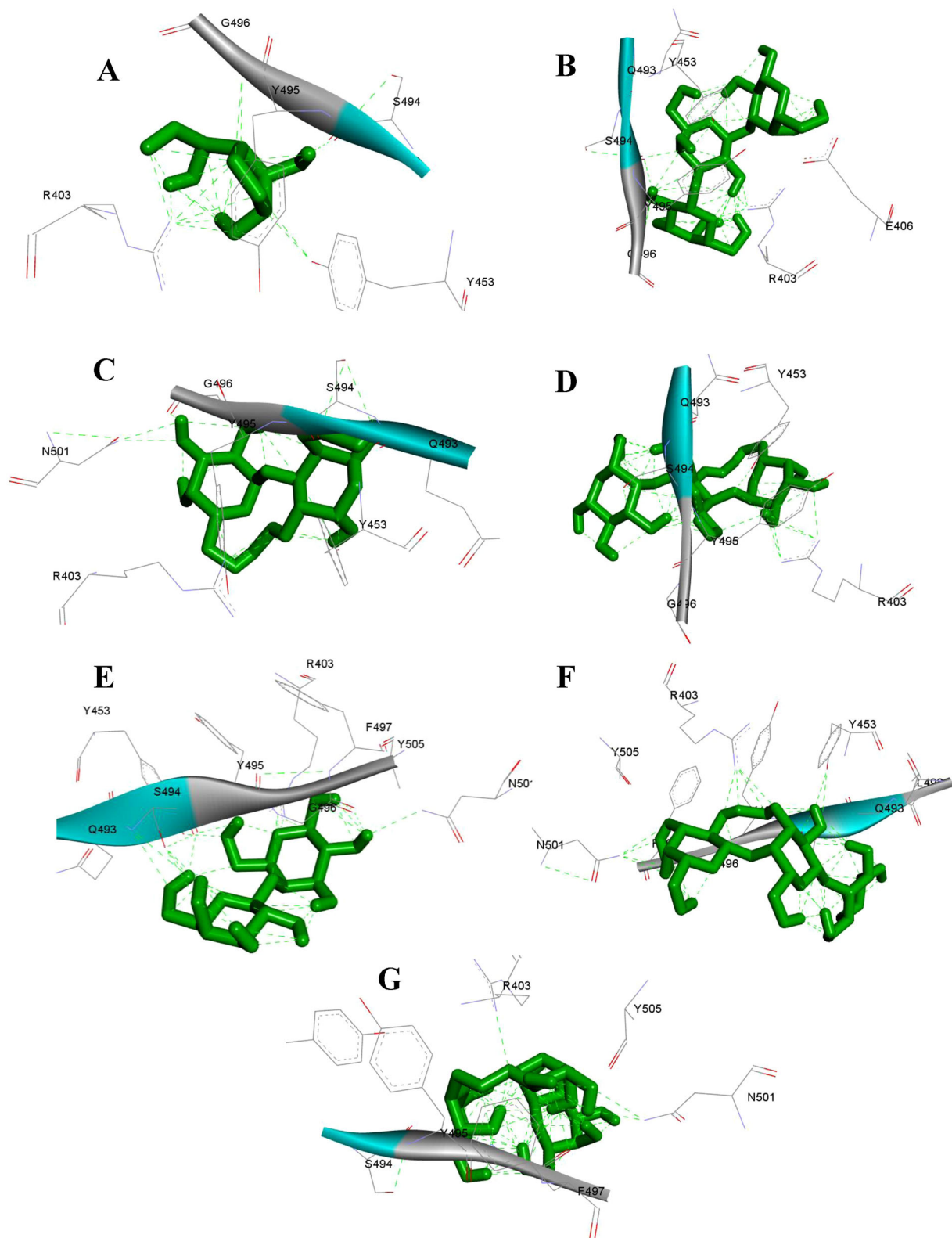
Figure 10. Molecular interaction of marine algal polysaccharides derivatives with 3CL^Pro of SARS-CoV-2. (A & B) The interaction of galactobiose with 3CL^Pro and their respective 2D structure; (C & D) The interaction of galactotriose with 3CL^Pro and their respective 2D structure; (E & F) The interaction of β-(1-6)-galactotriose with 3CL^Pro and their respective 2D structure.

hinder human visceral and cutaneous leishmaniasis (Moura et al., 2017) and defend malarial infection (Yilmaz et al., 2014). However, antiviral activity has not been reported so far for the foresaid carbohydrates. Thus, this study necessitates the *in vitro* and *in vivo* testing of these compounds since they had exhibited good interaction with the viral targets of SARS-CoV-2 over the commercial antiviral drugs and to unveil the mechanism of antiviral potential in the near future.

3.1.4. Seaweed polyphenols

Phlorotannins are classified under the polyphenolic compounds that are being considered as a suitable candidate for treating communicable and non-communicable diseases and their efficacy at the molecular level have not been elucidated in detail so far. Phlorotannins are secondary metabolites derived from brown algae, which are formed by polymerization of phloroglucinol monomer (1,3,5-trihydroxybenzene) through either ether, phenyl or 1,4-dibenzodioxin linkages.

Figure 11. Molecular interaction of marine algal polysaccharides derivatives with spike glycoprotein of SARS-CoV-2. (A) 3,6-anhydro-D-galactose; (B) β-(1-3)-galactotriose; (C) DialphaGal; (D) β-galactan; (E) Galactobiose; (F) Galactotriose; (G) β-(1-6)-galactotriose.

Phloroglucinol has been reported for anti-allergic, anti-inflammatory, anti-microbial, antioxidant and antiviral activities. It has also been reported to inhibit the reverse transcriptase and protease activities of HIV-1 (Kang et al., 2006). Besides, 8,8′-bieckol is an eckol type of phlorotannin that also has the efficiency in inhibiting the reverse transcriptase

activity in HIV-1 (Ahn et al., 2004). Eckol extracted from the brown alga *Ecklonia cava*, has been used as a tyrosinase inhibitor and docking of the tyrosinase-ligand complexed with eckol exhibited binding energy of −115.84 kcal/mol and found that eckol interacts with Asn205, His208 and Arg209 (Lee et al., 2015). Eckol was also identified as a possible
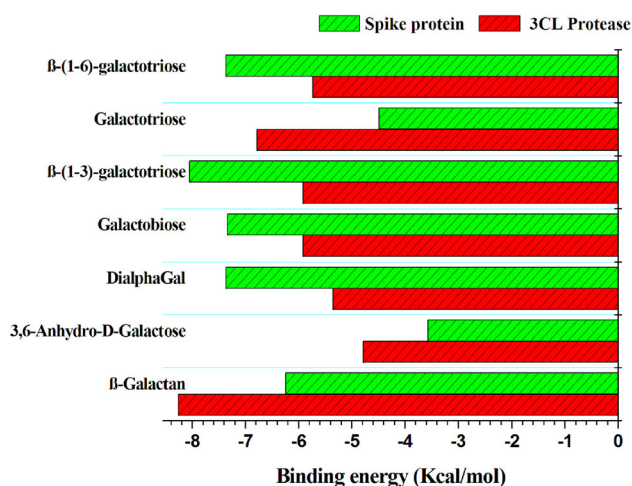
Figure 12. Comparative analysis of binding energies of polysaccharides derivatives with target proteins of SARS-CoV-2 (spike glycoprotein & 3CL^{Pro}).

therapy for neurodegenerative disorders targeting receptors of dopamine D3/D4. Eckol interacted hD3R with a binding energy (–6.41 kcal/mol), five H-bond interactions and hD4R with binding energy of (−6.46 kcal/mol), while the dopamine showed binding energy (–5.68 kcal/mol). This less binding energy may be due to four H-bond interactions, and eckol also formed hydrophobic and electrostatic interactions (Paudel et al., 2019).

Therefore, this study also explored the antiviral potentials of algal polyphenols like phloroglucinol, eckol, difucol and trifucol by computational analysis using the targets of SARS-CoV-2 (Figures 13 and 14). Similar to the above-mentioned results, eckol showed strong interaction with 3CL^{pro} with a higher binding energy of −8.19 kcal/mol with lower Ki of 993.73 nM (Table 4a), as compared to the docking score of COVID-19 experimental antiviral drugs such as dexamethasone, remdesivir, favipiravir and MIV-150. This result is clearly suggesting that eckol might be a promising drug for the treatment of COVID-19. Further, next to eckol the highest binding energy was obtained from trifucol with both the targets spike glycoprotein (−7.5 kcal/mol) and 3CL^{pro} (−6.3 kcal/mol), respectively (Table 4b and Figure 15). The other two ligands difucol and phloroglucinol had also shown good interaction with both the targets but whose biding energy and Ki are comparatively less to trifucol, eckol, dexamethasone and MIV-150.

### 3.1.5. SARS-CoV-2 experimental antiviral drugs

The antiviral potency of ligands through molecular docking is further validated by comparing the docking score of antiviral drugs (as positive controls), namely dexamethasone, remdesivir, favipiravir and MIV-150 by computational analysis. MIV-150 is reported as an anti-retroviral drug that is prepared with carrageenan as a drug delivery compound that can inhibit reverse transcriptase activity of HIV-1 (Singer et al., 2011). Among the positive controls, MIV-150 showed the highest binding energy with both spike glycoprotein and 3CL^{pro} of SARS-CoV-2 with the lowest Ki and highest hydrogen bond (Figures 16 and 17), whereas the interaction with the spike glycoprotein is relatively lesser than the 3CL^{pro}. And among the antiviral drugs used MIV-150 tops the chart with higher binding affinity and

lower Ki with both targets. Though it had been successful against other viral diseases, there is still no study on MIV-150's effect on SARS-CoV-2 both in vitro, in vivo and this is the first study to report MIV-150 against SARS-CoV-2 in silico. Therefore, this antiviral could be implemented for COVID-19 clinical trials since it had shown better docking scores as compared to recently tested anti-COVID-19 drugs dexamethasone, favipiravir and remdesivir.

Favipiravir (6-fluoro-3-hydroxy-2-pyrazine carboxamide) is reported as a broad-spectrum antiviral agent against different RNA viruses as it has the potential to inhibit the RNA-dependent RNA polymerase (RdRp) of RNA viruses (Furuta et al., 2017). Favipiravir has also shown good efficiency against influenza and Ebolavirus (Furuta et al., 2013; NIH, 2020; Oestereich et al., 2014). Recently, it was reported that favipiravir and remdesivir are potentially active and reducing the SARS-CoV-2 infection in vitro (EC$_{50}$ = 61.88 μmol/L, CC$_{50}$ > 400 μmol/L, SI > 6.46) (Wang et al., 2020). Additionally, favipiravir has been approved in Japan against novel epidemic influenza strains (Shiraki & Daikoku, 2020). In our study, the favipiravir showed a moderate interaction (Figure 18) with the targets and the highest hydrogen bond was observed in the interaction with 3CL^{pro} and spike glycoprotein. Remdesivir is a drug and used as a potent antiviral drug and reported to be effective against lethal Nipah and Ebola virus infections in nonhuman primates (Lo et al., 2019). It inhibits the replication of coronaviruses in respiratory epithelial cells, and the results obtained from this study indicate that the best binding energy and highest hydrogen bond with the targets of SARS-CoV-2 by remdesivir (Lo et al., 2019). Recently, dexamethasone is also been widely accepted as an antiviral drug for the treatment of COVID-19 patients. Dexamethasone was also used as a ligand for this study to perform the molecular docking with the SARS-CoV-2 targets. The results indicate that dexamethasone is a promising drug showing the highest binding energy with 3CL^{pro}, whereas its interaction with the spike glycoprotein is lesser (Table 5a,b).

Hence, the selected commercial antiviral drugs used for this in silico analysis had evidenced that the strong interaction with 3CL^{Pro}, which is highly essential for viral replication. Similarly, the ligands chosen from algal sources had also shown promising interaction with 3CL^{Pro} and spike glycoprotein than above-stated commercial antiviral drugs. Interestingly, we have observed that almost all the ligands had interacted by sulfuryl derivative and hydroxyl side chain with the targets of SARS-CoV-2. To the best of our knowledge, this is the first report to analyze the SARS-CoV-2 main target proteins binding affinity with β-galactan, alginate, galactotriose, β-(1,6)-galactotriose, 3,6-anhydro-D-galactose, β-galactan, dialphagal, β-(1-3)-galatotriose, galactobiose, α-carrageenan, 3,6-anhydro-D-galactose-2-sulfate, sulfoquinovosyl diaceylglycerol, difucol, trifucol and MIV-150.

Hence, this study would shed light on the discovery of potent biocompatible polysaccharides and its derivatives from algae as promising drug candidates against the severe COVID-19 pandemic. Further, this study proposes that these top-ranked bioactive compounds can be taken to next level of in vitro and preclinical studies to substantiate their potency in this crisis of search for antivirals.
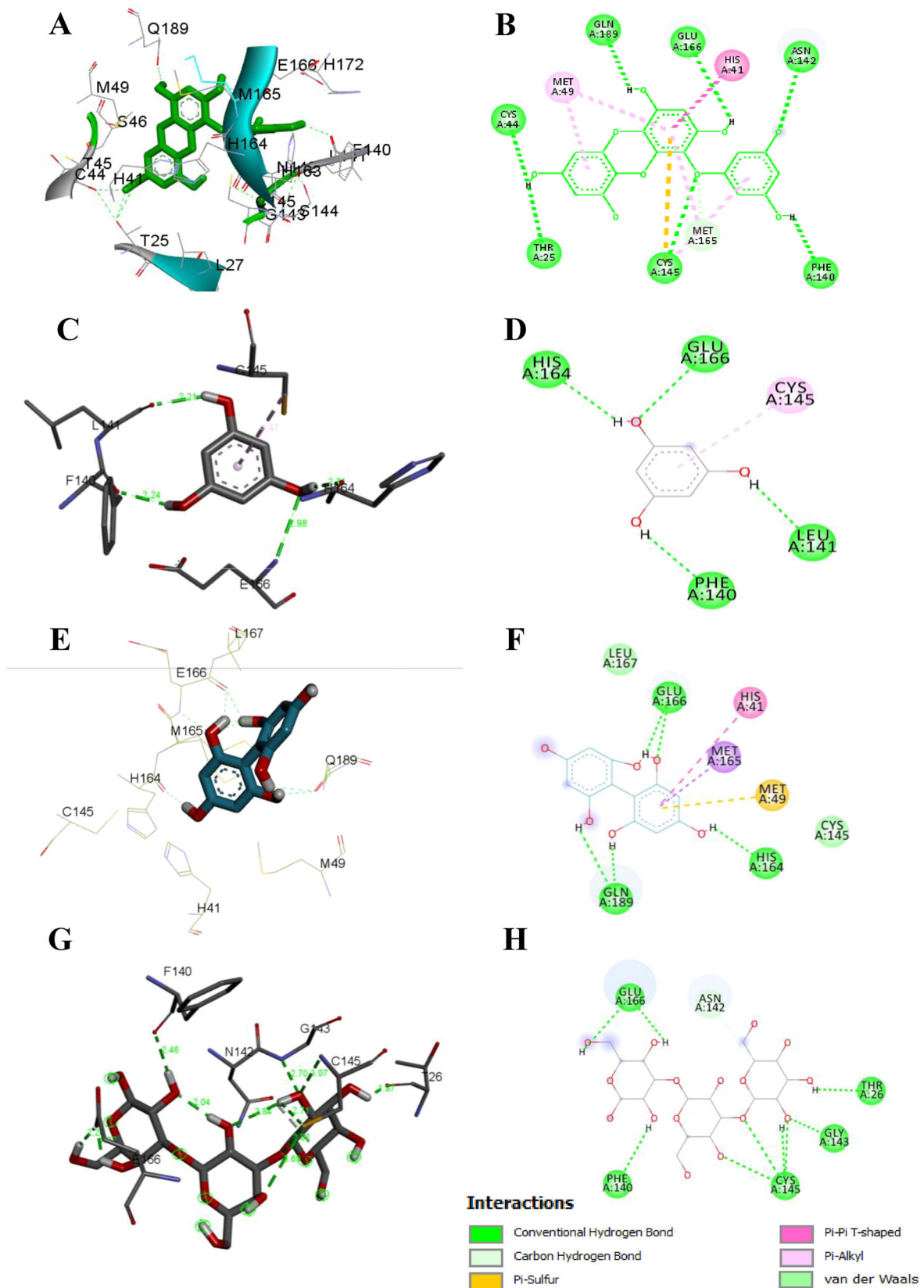
Figure 13. Molecular interaction of marine algal polyphenols with 3CL^Pro of SARS-CoV-2. (A & B) The interaction of eckol with 3CL^Pro and their respective 2D structure; (C & D) The interaction of phloroglucinol with 3CL^Pro and their respective 2D structure; (E & F) The interaction of difucol with 3CL^Pro and their respective 2D structure; (G & H) The interaction of trifucol with 3CL^Pro and their respective 2D structure.
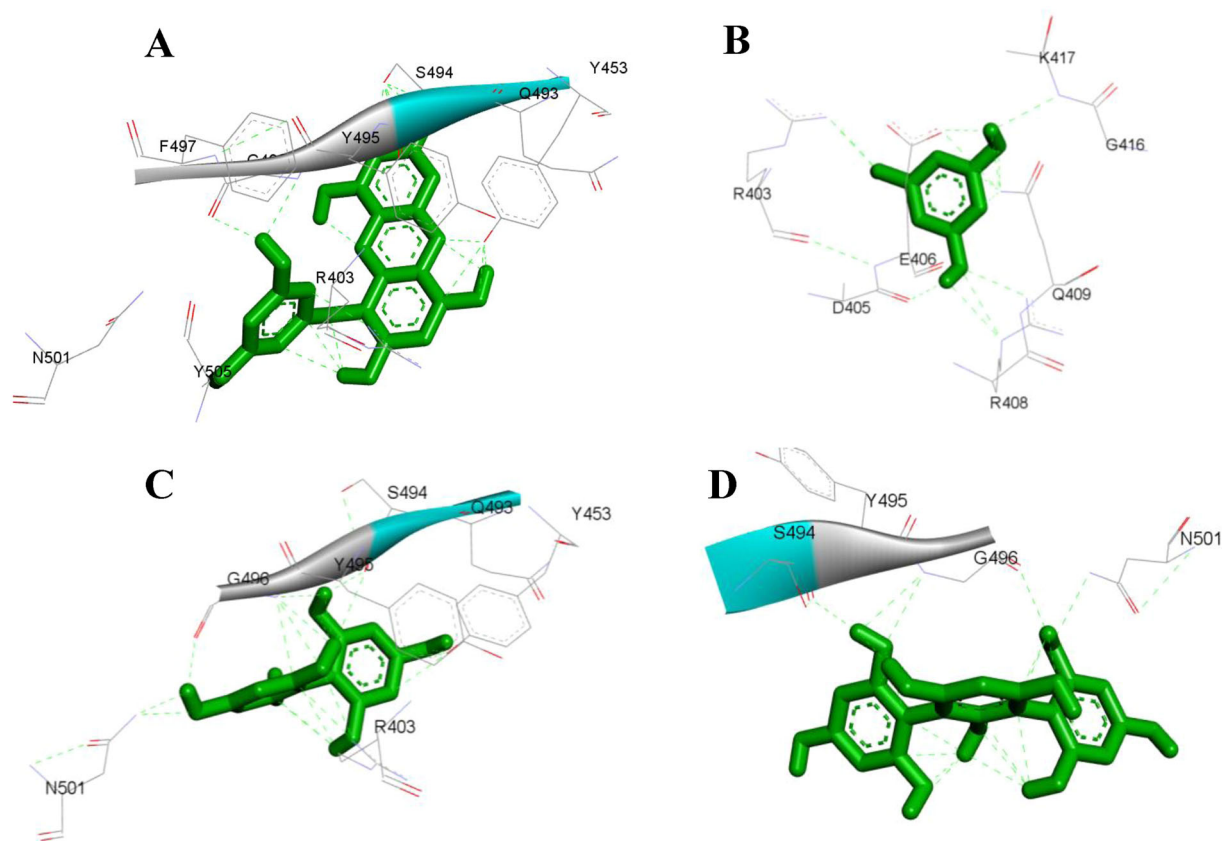
Figure 14. Molecular interaction of marine algal polyphenols with spike glycoprotein of SARS-CoV-2. (A) Eckol; (B) Phloroglucinol; (C) Difucol; (D) Trifucol.

Table 3a. Binding interaction parameters of marine algal polysaccharide derivatives with 3CL^{pro} protein target of SARS-CoV-2, where, Ki = inhibition constant, H = hydrogen bond and nH = non-hydrogen bond.

Compound name	PubChem CID	3CL Protease				
		Binding energy (kcal/mol)	Ki	Interactive residue	Bond type	Bond length (Å)
Galactobiose	448925	−7.33	4.24 μM	F140	H	2.62
				C145	H	2.87
				M165	nH	3.17
				E166	2H & nH	3.08, 2.10, 2.10
Galactotriose	448924	−4.49	511.27 μM	E166	2H & 2nH	2.86, 1.87, 2.77, 2.68
				H164	nH	3.25
				N142	2H	2.75, 2.91
β-(1,6)-galactotriose	51351734	−7.36	4.06 μM	E166	3H	2.17, 2.45, 2.13
				M165	2H	3.27, 2.95
				H164	H	2.48
3,6-anhydro-D-galactose	16069996	−4.78	313.14 μM	L141	H	1.78
				G143	H	3.40
				S144	H	1.88
				C145	H	3.33
				E166	2H	2.99, 2.09
β-galactan	53356679	−8.26	886.05 nM	L141	H	2.35
				N142	H	2.38
				E166	H	1.79
				Q189	H	2.82
DialphaGal	16219440	−7.26	4.75 μM	N142	2H & nH	3.05, 2.21, 3.46
				E166	H	3.11
				H164	H	2.66
				C145	2H	2.93, 2.53
β-(1-3)-galatotriose	51351759	−8.05	1.26 μM	T26	H	1.97
				F140	H	2.46
				N142	nH	3.67
				G143	H	2.70
				C145	4H	2.71, 2.92, 3.69, 3.07
				E166	2H	1.82, 2.20

Table 3b. Binding interaction parameters of marine algal polysaccharide derivatives with spike glycoprotein target of SARS-CoV-2, where, Ki = inhibition constant, H = hydrogen bond and nH = non-hydrogen bond.
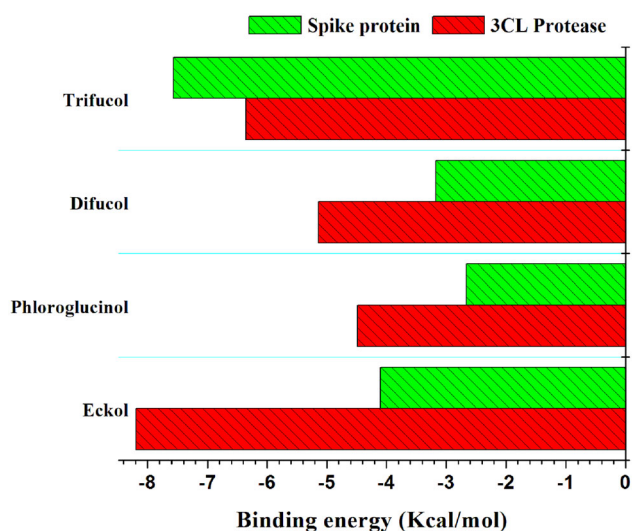
Compound name	PubChem CID	Binding energy (kcal/mol)	Ki	Interactive residue	Bond type	Bond length (Å)
Galactobiose	448925	−5.91	46.27 μM	R403	4nH	3.40, 4.44, 4.88, 4.76
				Y453	H	2.76
				S494	H & 2nH	3.17, 1.99, 1.85
				Y495	nH	2.55
				G496	2H & 2nH	2.91, 2.56, 2.13, 3.68
				N501	H	2.69
Galactotriose	448924	−6.78	10.68 μM	R403	2H & 7nH	2.94, 2.32, 4.20, 5.51, 3.87, 4.16, 4.65, 4.24, 5.53, 2.17
				Y453	nH	3.09
				Q493	nH	3.36
				Y495	nH	
β-(1,6)-galactotriose	51351734	−5.73	63.38 μM	G496	3H	2.21, 2.98, 2.87
				R403	2H & 5nH	3.03, 3.28, 5.19, 5.30, 4.40, 4.93, 4.12, 3.64
3,6-anhydro-D-galactose	16069996	−3.57	2.41 mM	S494	H	1.98
				Y495	H	3.17
β-galactan	53356679	−6.24	26.60 μM	R403	3H & 5nH	2.71, 2.94, 2.95, 1.93, 3.63, 3.83, 3.96, 4.41
				R403	3H	2.74, 3.09, 3.09
				Y453	4H	2.75, 3.10, 3.25, 3.35
				S494	H	2.24
				G496	H	3.29
DialphaGal	16219440	−5.35	119.23 μM	R403	H & 5nH	4.41, 3.21, 5.28, 4.77, 3.71, 4.80, 3.17
				Y453	H	3.09, 1.78, 1.91
				S494	H & 2nH	3.14, 1.92, 3.36
				G496	H & 2nH	
β-(1-3)-galatotriose	51351759	−5.91	46.41 μM	R403	4H	3.34, 3.39, 2.55, 2.95
				E406	nH	4.91
				Y453	3H & nH	3.36, 3.33, 3.06, 2.05
				S494	H	2.64
				G496	2H	3.27, 2.62

Table 4a. Binding interaction parameters of seaweed polyphenols with 3CL^pro protein target of SARS-CoV-2, where, Ki = inhibition constant, H = hydrogen bond and nH = non-hydrogen bond.

Compound name	PubChem CID	Binding energy (kcal/mol)	Ki	Interactive residue	Bond type	Bond length (Å)
Eckol	145937	−8.19	993.73 nM	T25	H	2.44
				H41	H	5.27
				C44	H	2.04
				M49	2H	4.67, 4.98
				F140	H	2.49
				N142	H	3.13
				C145	3H	3.23, 5.13, 5.61
				M165	2H	3.74, 4.80
				E166	H	2.51
				Q189	H	2.15
Phloroglucinol	359	−4.49	513.20 μM	F140	H	2.24
				L141	H	2.21
				C145	nH	4.47
				H164	H	2.31
				E166	H	2.98
Difucol	433697	−5.14	170.92 μM	H41	nH	5.74
				M49	nH	5.57
				Q189	2H & nH	2.00, 2.31, 1.32
				H164	H	2.01
				M165	2nH	3.94, 4.36
				E166	3H	1.91, 1.95, 2.71
Trifucol	71401226	−6.36	21.76 μM	T26	H	1.98
				H41	nH	5.82
				G143	H & nH	2.81, 2.59
				F140	H	2.06
				E166	H & nH	1.97, 2.37
				L141	nH	3.86
				N142	nH	2.23
				G143	H & nH	2.50, 2.81
				C145	H & 2nH	2.59, 3.52, 5.82

Table 4b. Binding interaction parameters of seaweed polyphenols with spike glycoprotein target of SARS-CoV-2, where, Ki = inhibition constant, H = hydrogen bond and nH = non-hydrogen bond.

Compound name	PubChem CID	Binding energy (kcal/mol)	Ki	Interactive residue	Bond type	Bond length (Å)
					Spike Glycoprotein	
Eckol	145937	−4.10	982.86 μM	R403	H	3.44
				Y453	2H	2.17, 3.03
				S494	3H	1.99, 2.63, 2.88
Phloroglucinol	359	−2.66	11.16 mM	R403	H	2.90
				D405	nH	2.15
				E406	5nH	2.20, 2.96, 3.72, 4.59, 4.98
						2.73
				Q409	H	2.90
				K417	H	
Difucol	433697	−3.17	4.73 mM	N501	H	2.56
				R403	2H & 8nH	2.73, 2.88, 3.66, 3.13, 3.83, 4.65, 4.77, 5.38, 3.47, 4.94
						2.70, 2.99, 2.15
				G496	2H & nH	2.64
				Y495	nH	3.12, 5.91
				Y453	H & nH	3.15, 1.89
				S494	H & nH	
Trifucol	71401226	−7.57	2.85 μM	R403	nH	5.58
				N501	H	3.19
				S494	H	1.99
				G496	H	2.39

Figure 15. Comparative analysis of binding energies of seaweed polyphenols with target proteins of SARS-CoV-2 (spike glycoprotein & 3CL^Pro).

3.2. Molecular dynamics simulation

To further validate the molecular docking findings, the MD simulation was performed for the SARS-CoV-2 main protease with selected lead marine algal compounds to evaluate the structural stability and constancy of macromolecule interactions with the ligand by Desmond tool. MD simulation system was prepared for 3CL^pro of SARS-CoV-2 with potent marine algal inhibitors to find out the strong interactions based on hydrogen bonds, hydrophobic, ionic and water bridges. The MD simulation provides information on the position and distance patterns of the interacting amino acids to build a stable inhibition complex. In Figure 19, the Root Mean Square Deviation (RMSD) value is shown from the simulation results. The changes of RMSD value throughout the simulation time for both the ligand and the macromolecule were around 3 Å, which testify the stability of the complex. The Root Mean Square Fluctuation (RMSF) of the macromolecule-ligand complex is illustrated in Figures 20 and S4. In an efficient macromolecule-ligand association, a

Table 5a. Binding interaction parameters of commercial COVID-19 experimental antiviral drugs with 3CL^pro protein target of SARS-CoV-2, where, Ki = inhibition constant, H = hydrogen bond and nH = non-hydrogen bond.

Compound name	PubChem CID	Binding energy (kcal/mol)	Ki	Interactive residue	Bond type	Bond length (Å)
					3CL Protease	
MIV-150	9907284	−7.57	2.80 mM	E166	3H	1.94, 2.10, 3.35
Remdesivir	121304016	−6.82	10.04 μM	N142	H	2.94
				L141	H	3.61
				C145	2H	3.06, 3.09
				H164	2H	2.89, 3.22
				M165	H	2.73
				M49	nH	4.29,
				P168	nH	4.76
				Q198	nH	3.53
Favipirivir	492405	−4.01	1.15 mM	E166	2H	2.41, 3.21
				F140	H	2.29
				L141	3H	2.62, 2.62, 2.62
				S144	2H	1.93, 3.09
				C145	H	2.47
Dexamethasone	5743	−7.19	5.40 μM	E166	H & nH	1.68, 3.02
				Q189	H	3.17
				S144	H	2.92

Table 5b. Binding interaction parameters of commercial COVID-19 experimental antiviral drugs with spike glycoprotein target of SARS-CoV-2, where, Ki = inhibition constant, H = hydrogen bond and nH = non-hydrogen bond.

Compound name	PubChem CID	Spike Glycoprotein				
		Binding energy (kcal/mol)	Ki	Interactive residue	Bond type	Bond length (Å)
MIV-150	9907284	−5.07	192.49 μM	D405	H	2.93
				Y508	3H & 4nH	2.76, 3.23, 3.60, 4.86, 4.08, 3.99, 4.26 4.11, 5.44
				B407	2nH	4.90
				R408	nH	
Remdesivir	121304016	−3.87	1.47 mM	S494	3H	1.86, 2.36, 252
				R403	3H	3.28, 3.06, 3.34
				496	nH	3.55
				Y453	2nH	3.35, 5.06
Favipirivir	492405	−3.53	2.59 mM	R403	2H & nH	2.92, 3.34, 3.03
				Y505	2H	2.12, 2.36
				N501	2H	2.36, 2.12
				G496	2H	2.97, 2.98
Dexamethasone	5743	−4.35	652.16 μM	Y421	2nH	4.72, 4.69
				E406	H & 3nH	2.95, 5.52, 4.90, 4.34
				R403	2H & 2nH	2.96, 3.29, 3.27, 5.55
				Q493	H	3.36
				Y453	2H	3.40, 3.29
				R454	H	2.60

combination of all the interactions in the allosteric site profoundly supports a stable strong interaction. In Figure S3 all interactions across the simulation are shown such as protein-ligand contacts timeline, protein secondary structure elements (SSE) like alpha-helices and β-strands which were monitored throughout the simulation.

In simulation studies, the ligand-macromolecule complex maintained a stable interaction, which should present at least 30% of the total simulation time. Eckol showed polar interaction with Asn 142 at 33% of simulation time; while charged interaction with Glu 166 was 59% of the simulation time. Here, Glu 166 exhibited the highest number of hydrogen bonds as well as water bridges. Similarly, in β-galactan, ligand-interaction patterns showed the polar contacts with Gln 192, Thr 190 and His 64, where the interaction time was 61%, 41% and 64%, respectively. Here also, along with polar contacts, charged contacts on Asp 187 and Glu 166 displayed 48% and 73% of total interaction time, respectively. Glu 166 and Gln 192 showed more hydrogen bonds with water bridges. In addition, β-carrageenan showed strong hydrogen bonds with Gly 142, Ser 143, Cys 144, Asp 145 and Arg 189. β-glucan showed multiple contacts in hydrogen bond with Tyr 54, Glu 166 and Asn 214. Laminarin showed hydrogen bonding in Ser 46, Glu 47, Asp 48, Glu 166 and Gln 189 with water bridges. Here, charged contact with Glu 166 was maintained throughout 34% of simulation time while the polar charge on Ser 46, Gln 189 were maintained for 34% and 31% of interaction time, respectively.

In MD study, the total time trajectory was up to 200 ns, where eckol showed continuous contact with Glu 166, Asn 142, His 41 and Thr 26 and time-variable contact with Gln 189, Pro 168, Met 165, Cys 44. β-galactan showed continuous contacts with Glu 166 and shift in Cyt 145, His 164, Thr 190 and Gln 192 with variation in time. In β-(1,6)-galactotriose, Glu 166, Gln 189, Asn 142 showed interactions with variation in time, contact shifts to Asp 155, 153 and Asp 248. β-(1-3)-galatotriose showed various hydrogen bonds and contact variation shift in Gln 189, Gly 183, Glu 240 and Lys 102, Arg 105, etc. β-carrageenan showed contacts in Glu 166, Cys

145, Asn 142 shift to Ala 194 and Asp 229. β-Glucan presented strong contacts with Glu 166 with the shift to Val 25, Glu 55 and Asn 214. Laminarin showed affinity with Gln 189, Glu 166, Cyt 145, Ser 46 with the shift to Glu 47, Asp 48.

Among all simulation results, Glu 166 showed the highest number of hydrogen bonds with water bridges and conserved in all dynamics studies than Gln 189. So, among the total interaction, Glu 166 and Gln 189 held a strong binding affinity to the ligands. An adequate protein-ligand association indicated a stable complex formation, in sight of all the interaction in the allosteric region. Further, *in vitro* and *in vivo* validations of these algal compounds are needed to prove its efficacy against COVID-19 in near future.

3.3. DFT – Quantum chemical calculations

DFT analysis can render valuable insights into the structure-activity relation of molecules by analyzing the molecular structure using the energies of their molecular orbitals (Geerlings et al., 2020). The conceptual prediction of structural and iso-density properties of the compounds was given in Figure S5. Since the electron transfer mechanism is one of the fundamental phenomena for the enzymatic reactivity. The frontier orbital was determined by the energy gap between the highest occupied molecular orbital (HOMO) and lowest unoccupied molecular orbital (LUMO) of the compounds. The HOMO indicates the electron donor properties, whereas the LUMO indicates electron-accepting properties. Recently, quantum chemical calculation has been used to investigate the structural properties and realistic potential of the compounds against biomolecules. The energy level of the ground state and excitation state of the molecules were tabulated in Table 6. The ΔE is comparatively lower in κ-carrageenan (1.47 eV), whereas the higher energy gap of the investigated compound was β-1,3-galactotriose (7.02 eV). However, the other compound also exhibits almost the same level of energy gap shown in Figure 21. Additionally, the global hardness, softness electronegativity and electrophilicity were also examined to investigate the cell permeability of the molecules (Majumdar et al., 2020). Especially, global softness is one
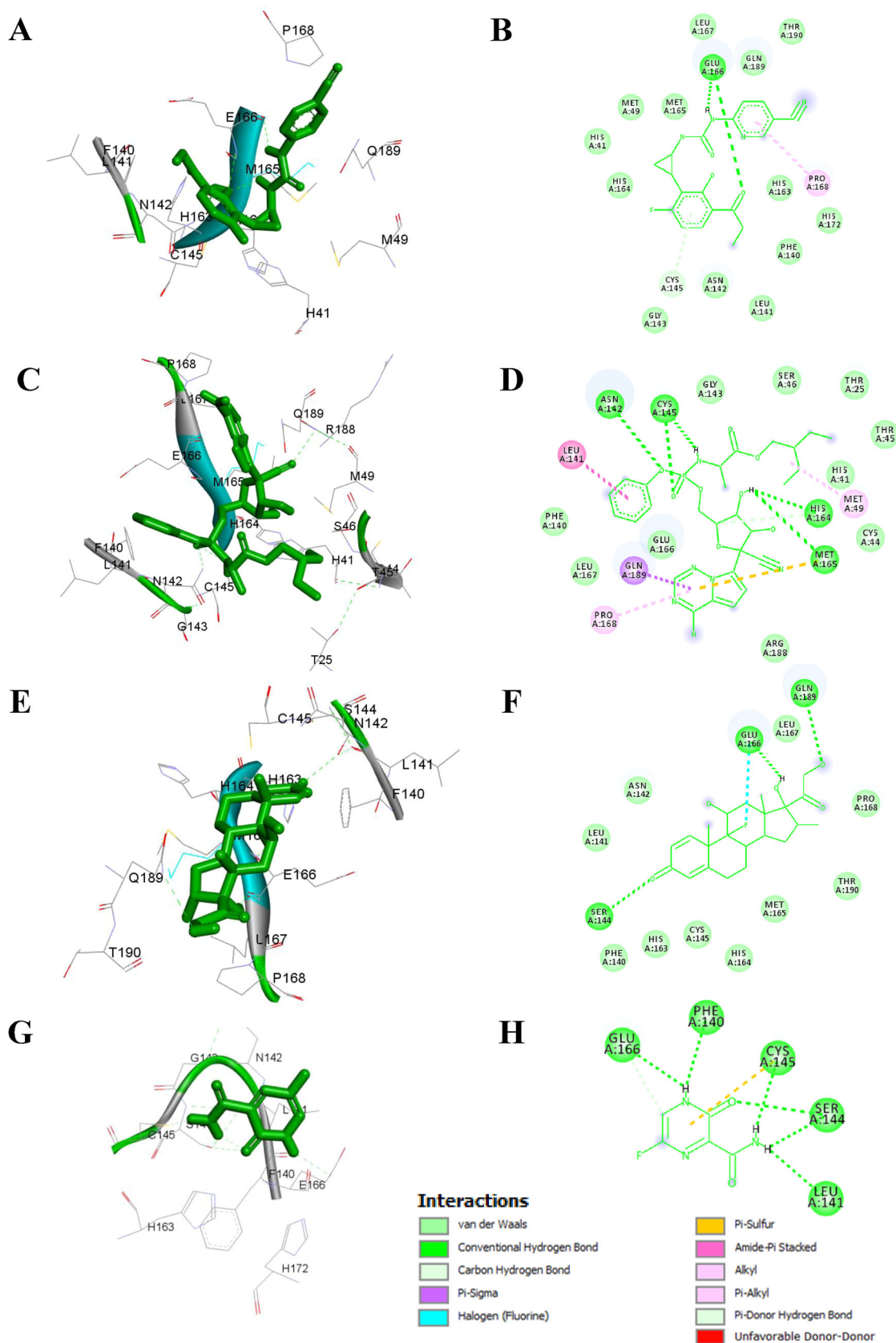
Figure 16. Molecular interaction of commercial COVID-19 experimental antiviral drugs with 3CL^Pro of SARS-CoV-2. (A & B) The interaction of MIV-150 with 3CL^Pro and their respective 2D structure; (C & D) The interaction of Remdesivir with 3CL^Pro and their respective 2D structure; (E & F) The interaction of Dexamethasone with 3CL^Pro and their respective 2D structure; (G & H) The interaction of Favipiravir with 3CL^Pro and their respective 2D structure.
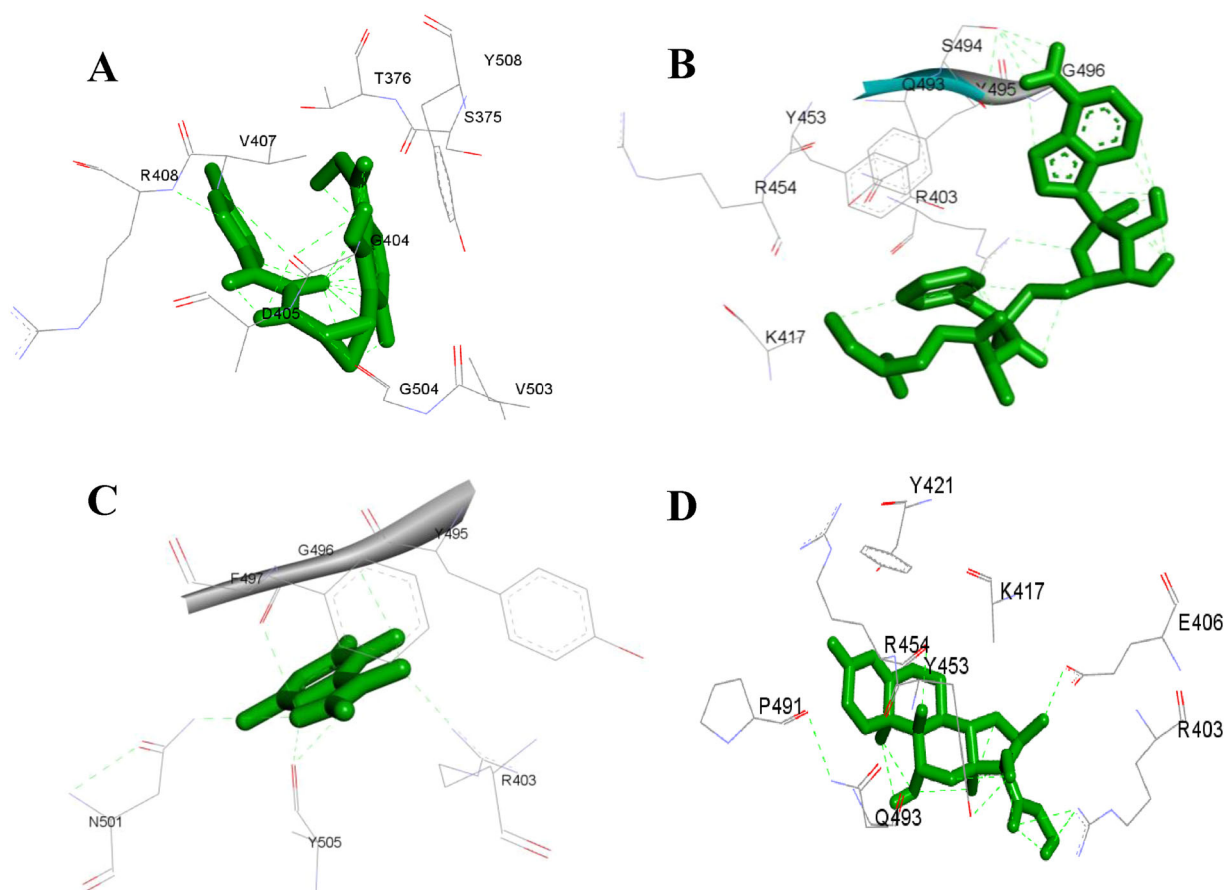
Figure 17. Molecular interaction of commercial COVID-19 experimental antiviral drugs with spike glycoprotein of SARS-CoV-2. (A) MIV-150; (B) Remdesivir; (C) Dexamethasone; (D) Favipiravir.
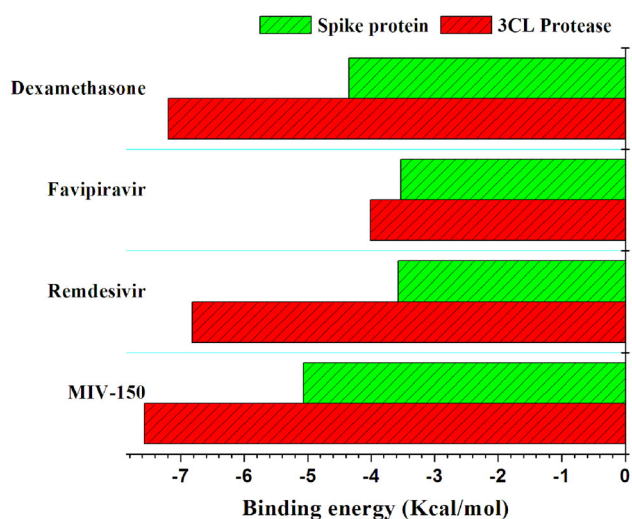

Figure 18. Comparative analysis of binding energies of commercial COVID-19 experimental antiviral drugs with SARS-CoV-2 targets (spike glycoprotein & 3CL^{Pro}).

of the important criteria that facilitate the permeability of mammalian cells. The κ-carrageenan possessed higher softness and electrophilicity as compared with other compounds (Table 6). These results suggest that the binding affinity of the drug toward electrocharged biomolecules could efficiently interact in the aspect of a quantum chemical reaction.

## 3.4. Pharmacokinetics and metabolic properties of ligand molecules by ADMET profiling

To further validate the marine algal compounds for drug-likeliness, the parameters such as absorption, distribution, metabolism, excretion and toxicity (ADMET) profile were investigated. ADMET properties are consideredto be the crucial parameters for drug-likeness evaluation in the early drug discovery process. The major two determinants such as solubility and permeability are very important in the metabolism of drugs. In the present study, the prediction of ADMET, pharmacokinetics, drug-likeness properties of the marine algal compounds was evaluated *in silico* by Schrodinger's QikProp module. The ADMET studies were performed for the ligand molecules which exhibited higher potential inhibition against 3CL protease and spike protein of SARS-CoV-2. The major ADMET properties for drug-likeness were predicted (serially numbered in Tab. 7) such as 1. molecular weight of the molecule (mol_MW); 2. dipole moment of the molecule; 3, 4. Estimated number of hydrogen bonds that would be accepted/donated by the solute from/to water molecules in an aqueous solution (donorHB/accptHB); 5. Predicted polarizability in cubic angstroms (QPpolrz); 6. Predicted water/gas partition coefficient (QPlogPw); 7. Predicted octanol/water partition coefficient (QPlogPo/w); 8. Predicted aqueous solubility (QPlogS); 9. Predicted IC$_{50}$ value for blockage of HERG K$+$ channels (QPlogHERG); 10. Predicted apparent Caco-2 cell permeability-model for the gut-blood barrier (QPPCaco); 11. Predicted brain/blood partition coefficient (QPlogBB); 12. Predicted skin
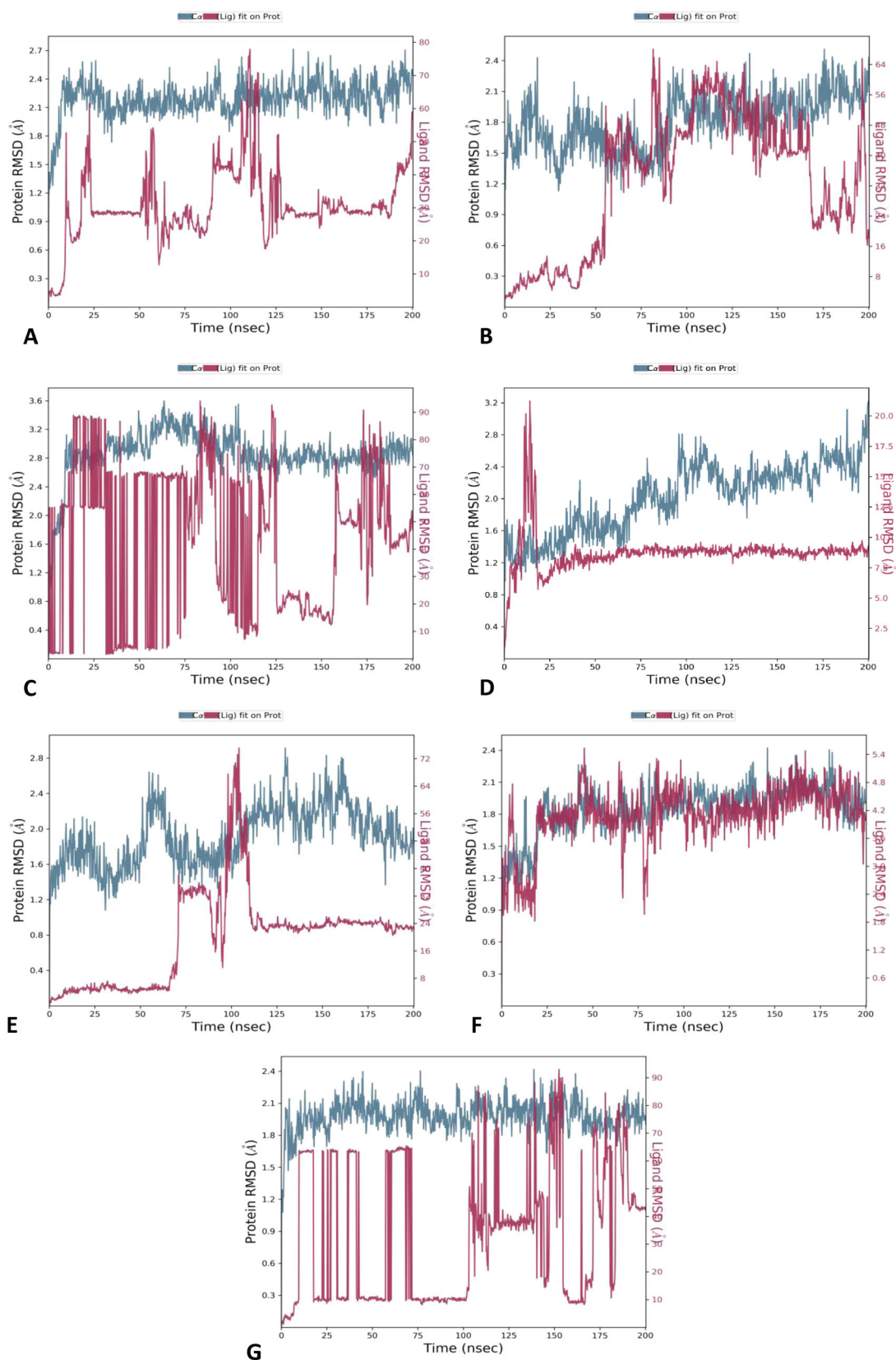
Figure 19. Time evolution of RMSD (root mean square deviations) values during the simulation of 3CL^{pro} complex with (A). β-(1-3)-galactotriose; (B). β-(1-6)-galactotriose; (C). β-carrageenan; (D). β-galactan; (E). β-glucan; (F). Eckol; (G). Laminarin.

permeability (QPlogKp); 13. The number of likely metabolic reactions (#metab); 14. Prediction of binding to human serum albumin (QPlogKhsa); 15, 16. Predicted qualitative human oral absorption based on the set of rules, including the number of metabolites, number of rotatable bonds, logP, solubility and cell permeability; 17. Van der Waals surface area of polar oxygen and
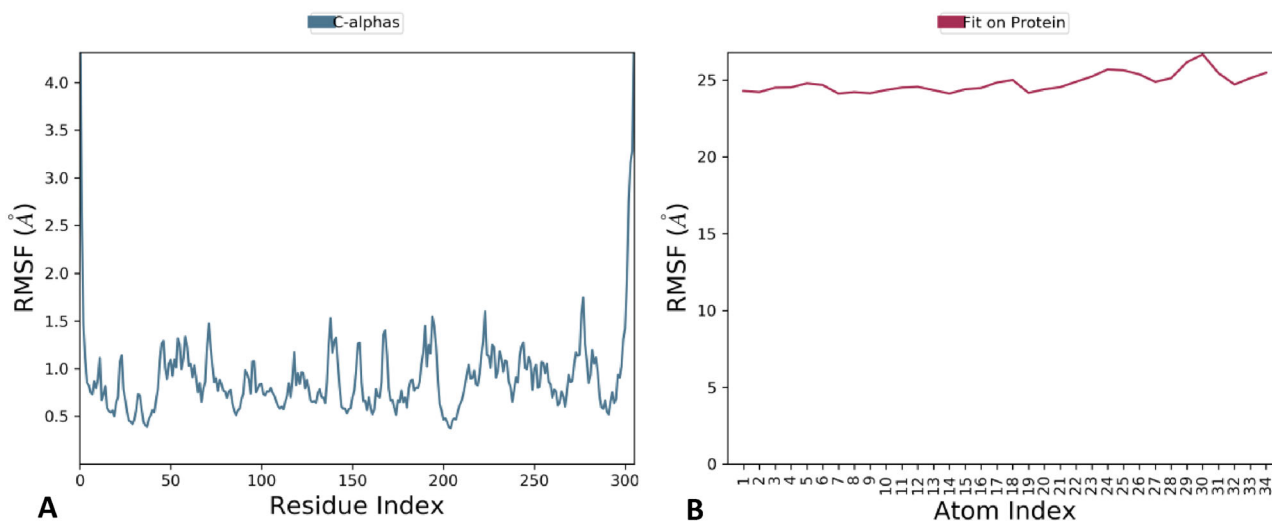
Figure 20. RMSF (Root mean square fluctuations) of C_α atoms of $3CL^{pro}$ complex with ligand β-(1-3)-galactotriose. Other ligands are mentioned in Supplementary Figure 4.

Table 6. The energy level of the ground state and excitation state of the top-ranked marine algal compounds.

S. No.	Compound name	Hartree atomic units		E_{HOMO} (eV)	E_{LUMO} (eV)	ΔE_g (eV)	χ	η	Δ	ω
		HOMO	LUMO							
1	β-1,3-galactotriose	0.2660	0.0045	7.1456	0.1224	7.0231	3.6340	3.5116	0.2847	1.8804
2	β-carrageenan	0.2585	0.0198	7.0351	0.5398	6.4952	3.7875	3.2476	0.3079	2.2085
3	Dialphagal	0.2632	0.0188	7.1630	0.5123	6.6506	3.8377	3.3253	0.3007	2.2145
4	Eckol	0.2032	0.0244	5.5292	0.6661	4.8631	3.0977	2.4316	0.4112	1.9731
5	κ-carrageenan	0.2429	0.1888	6.6108	5.1379	1.4728	5.8743	0.7363	1.3580	23.4324
6	Laminarin	0.2561	0.0097	6.9698	0.2655	6.7042	3.6177	3.3521	0.2983	1.9521
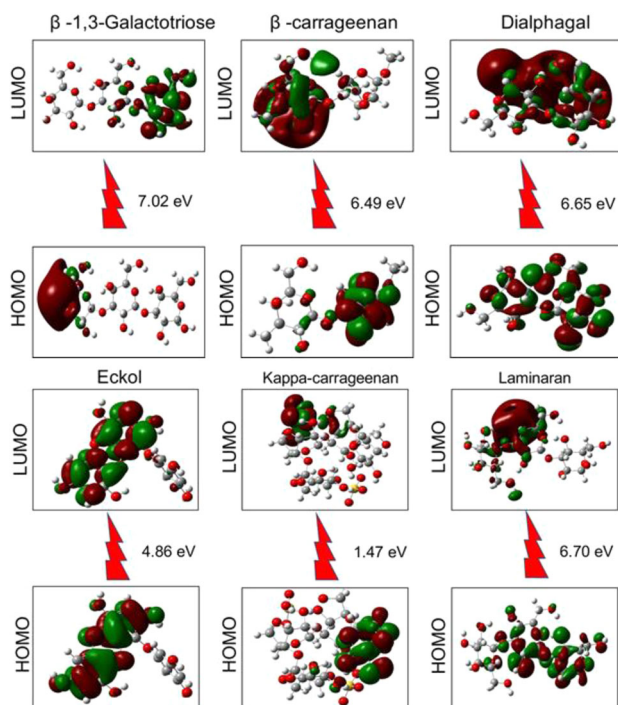
Figure 21. The energy level of Frontier molecular orbitals (FMOs) of marine algal compounds.

nitrogen atoms (PSA); 18. The number of violations of Lipinski's rule of five (RuleOfFive) and compounds with mol_MW < 500, QPlogPo/w < 5, donorHB $\leq$ 5, accptHB $\leq$ 10 are considered druglike; 19. Number of violations of Jorgensen's rule of three

(RuleOfThree). The compounds with lower violations of the following parameters such as QPlogS > −5.7, QP PCaco > 22 nm/s, # Primary Metabolites < 7 are more likely to be orally available; 20. Predicted maximum transdermal transport rate (Jm). The results obtained were compared with the reference values of the QikProp 3.5 User Manual to predict physically significant descriptors and pharmaceutically relevant properties of organic molecules (QikProp, version 3.5., Schrödinger).

The top-ranked marine algal compounds (β-(1-6)-galactotriose, β-(1-3)-galactotriose, eckol, β-glucan and laminarin) from molecular docking studies satisfied most of the drug-like properties and ADMET profile. Especially 4 out of 6 ligands exhibited great scope in rules of five and rules of three. The β-(1-6)-galactotriose, β (1-3)-galactotriose and laminarin ligand molecules were in the recommended range at 3 in the rule of five and greater than 1 in the rules of three thus revealing promising drug-likeliness property as well imitating as equivalent to commercially available drugs. Other major characteristic features like human oral adsorption, cell permeability, metabolic reaction index, skin permeability, blood-brain barrier and partition co-efficiency were seemed to be of greater value which substantiates the drug-like behavior of the ligand molecules which can be considered as algal lead compounds against COVID-19. Thus, it can be concluded that these compounds can be taken up for the next level of *in vivo* and preclinical investigations in order to prove their efficacy against SARS-CoV-2 infection.

Table 7. Physically significant descriptors and pharmaceutically relevant properties for drug-likeness of top-ranked marine algal compounds.

S. No.	Parameters (Range)	Compounds					
		β-(1-6)-galatotriose	β-(1-3)-galatotriose	β-carrageenan	β-glucan	Eckol	Laminarin
1	mol_MW (130.0–725.0)	504.441	504.441	336.338	370.353	390.43	504.441
2	dipole (1.0–12.5)	12.743	10.824	3.989	8.219	3.357	4.893
3	donorHB (0.0–6.0)	11	11	4	6	6	11
4	accptHB (2.0–20.0)	27.2	27.2	15.3	18.7	15.3	27.2
5	Qppolrz (13.0–70.0)	39.035	36.635	28.004	29.342	34.693	35.679
6	QPlogPw (4.0–45.0)	43.727	43.295	21.322	27.391	25.066	43.024
7	QPlogPo/w (−2.0–6.5)	−6.214	−5.85	−1.626	−2.874	−1.575	−5.628
8	QPlogS (−6.5–0.5)	−1.073	−0.815	−1.318	−1.054	−2.312	−0.784
9	QPlogHERG (below −5)	−5.411	−4.577	−3.763	−3.952	−3.932	−4.378
10	QPPCaco (below 25 poor; above 500 great)	0.41	0.938	284.545	46.268	35.488	1.926
11	QPlogBB (−3.0–1.2)	−5.853	−4.814	−1.377	−2.425	−2.289	−4.363
12	QPlogKp (−8.0–1.0)	−8.31	−7.612	−3.748	−4.897	−5.505	−7.004
13	#metab (1–8)	10	10	5	6	9	10
14	QPlogKhsa (−1.5–1.5)	−2.464	−2.156	−1.308	−1.548	−0.978	−2.079
15	Human Oral Absorption (1–3)	1	1	2	2	2	1
16	Percent Human Oral Absorption (above 80% is high below 25% is poor)	0	0	61.352	14.006	32.506	0
17	PSA (7.0–200.0)	278.506	273.274	124.483	168.739	152.839	266.835
18	Rules of Five	3	3	0	2	1	3
19	Rules of Three	2	2	0	0	1	2
20	Jm (Kp × MW × S ($\mu g\ cm^{-2}\ h^{-1}$))	0	0.002	2.889	0.415	0.006	0.008

4. Conclusion

The computational approaches for virtual screening of the natural compounds of marine algae retrieved from the PubChem database were docked with the spike glycoprotein and 3CL^{pro} of the novel SARS-CoV-2 to investigate the ability of the compounds to block the entry of the virus by preventing the attachment and its replication. The docking results attained are strongly suggesting that the algal sulfated polysaccharides, polysaccharides derivatives and polyphenols exhibited a better interaction with both targets of SARS-CoV-2 when compared to commercial leading antiviral drugs against COVID-19. Moreover, the validations of the lead marine algal compounds obtained from molecular docking were further substantiated by molecular dynamic simulation, DFT calculations and ADMET profiling. Therefore, based on the mechanism of interaction of these ligands with the viral targets, it can be further evaluated by conducting *in vitro* and clinical studies to confirm their antiviral activity against SARS-CoV-2 and these compounds would be suitable drug candidates for the treatment of the COVID-19 pandemic situation in near future.

Disclosure statement

The authors declare no conflict of interest.

ORCID

Perumal Varalakshmi http://orcid.org/0000-0002-5420-4688

References

Abdel-Motal, U. M., Wang, S., Awad, A., Lu, S., Wigglesworth, K., & Galili, U. (2010). Increased immunogenicity of HIV-1 p24 and gp120 following immunization with gp120/p24 fusion protein vaccine expressing α-gal epitopes. *Vaccine*, *28*(7), 1758–1765. https://doi.org/10.1016/j.vaccine.2009.12.015

Ahmadi, A., Zorofchian, M. S., Abubakar, S., & Zandi, K. (2015). Antiviral potential of algae polysaccharides isolated from marine sources: A review. *BioMed Research International*, *2015*, 1–10. https://doi.org/10.1155/2015/825203

Ahn, M.-J., Yoon, K.-D., Min, S.-Y., Lee, J. S., Kim, J. H., Kim, T. G., Kim, S. H., Kim, N.-G., Huh, H., & Kim, J. (2004). Inhibition of HIV-1 reverse transcriptase and protease by phlorotannins from the brown alga Ecklonia cava. *Biological and Pharmaceutical Bulletin*, *27*(4), 544–547. https://doi.org/10.1248/bpb.27.544

Baba, M., Schols, D., De Clercq, E., Pauwels, R., Nagy, M., Gyorgyi-Edelenyi, J., Low, M., & Gorog, S. (1990). Novel sulfated polymers as highly potent and selective inhibitors of human immunodeficiency virus replication and giant cell formation. *Antimicrobial Agents and Chemotherapy*, *34*(1), 134–138. https://doi.org/10.1128/AAC.34.1.134

Barbosa, J. D. S., Costa, M. S. S. P., Melo, L. F. M. D., Medeiros, M. J. C. D., Pontes, D. D. L., Scortecci, K. C., & Rocha, H. A. O. (2019). Caulerpa Cupressoides Var. Flabellata. *Marine Drugs*, *17*(2), 105. https://doi.org/10.3390/md17020105

Bi, D., Yu, B., Han, Q., Lu, J., White, W. L., Lai, Q., Cai, N., Luo, W., Gu, L., Li, S., Xu, H., Hu, Z., Nie, S., & Xu, X. (2018). Immune activation of RAW264.7 macrophages by low molecular weight fucoidan extracted from New Zealand Undaria pinnatifida. *Journal of Agricultural and Food Chemistry*, *66*(41), 10721–10728. https://doi.org/10.1021/acs.jafc.8b03698

Biovia, D. (2016). *Discovery Studio Modeling Environment, Release 2017*. DassaultSystèmes. http://AccelrysCom/Products/Collaborative-Science/Biovia-Discoverystudio/Visualization Download Php 2016.

Cascella, M., Rajnik, M., Cuomo, A., Dulebohn, S. C., & Di Napoli, R. (2021). Features, evaluation and treatment coronavirus (COVID-19). In *StatPearls*. StatPearls Publishing.

Chan, J. F. W., To, K. K. W., Tse, H., Jin, D. Y., & Yuen, K. Y. (2013). Interspecies transmission and emergence of novel viruses: Lessons from bats and birds. *Trends in Microbiology*, *21*(10), 544–555. https://doi.org/10.1016/j.tim.2013.05.005

Chen, N., Zhou, M., Dong, X., Qu, J., Gong, F., Han, Y., Qiu, Y., Wang, J., Liu, Y., Wei, Y., Xia, J., Yu, T., Zhang, X., & Zhang, L. (2020). Epidemiological and clinical characteristics of 99 cases of 2019 novel coronavirus pneumonia in Wuhan, China: A descriptive study. The Lancet, 395(10223), 507–513. https://doi.org/10.1016/S0140-6736(20)30211-7

Chiba, S., Ikushima, H., Ueki, H., Yanai, H., Kimura, Y., & Hangai, S. (2014). Recognition of tumor cells by Dectin-1 orchestrates innate immune cells for anti-tumor responses. ELife, https://doi.org/10.7554/eLife.04177

Damonte, E. B., Matulewicz, M. C., & Cerezo, A. S. (2004). Sulfated seaweed polysaccharides as antiviral agents. Current Medicinal Chemistry, 11(18), 2399–2419. https://doi.org/10.2174/0929867043364504

De Souza, L. M., Sassaki, G. L., Romanos, M. T. V., & Barreto-Bergter, E. (2012). Structural characterization and anti-HSV-1 and HSV-2 activity of glycolipids from the marine algae Osmundaria obtusiloba isolated from Southeastern Brazilian coast. Marine Drugs, 10(12), 918–931. https://doi.org/10.3390/md10040918

DeLano, W. L. (2014). The PyMOL Molecular Graphics System, Version 1.8. Schrödinger LLC.

Delattre, C., Fenoradosoa, T. A., & Michaud, P. (2011). Galactans: An overview of their most important sourcing and applications as natural polysaccharides. Brazilian Archives of Biology and Technology, 54(6), 1075–1092. https://doi.org/10.1590/S1516-89132011000600002

Dictionary of Food Compounds with CD-ROM. (2013). Choice Reviews Online. https://doi.org/10.5860/choice.51-1824

Drosten, C., Günther, S., Preiser, W., van der Werf, S., Brodt, H.-R., Becker, S., Rabenau, H., Panning, M., Kolesnikova, L., Fouchier, R. A. M., Berger, A., Burguière, A.-M., Cinatl, J., Eickmann, M., Escriou, N., Grywna, K., Kramme, S., Manuguerra, J.-C., Müller, S., … Doerr, H. W. (2003). Identification of a novel coronavirus in patients with severe acute respiratory syndrome. New England Journal of Medicine, 348(20), 1967–1976. https://doi.org/10.1056/NEJMoa030747

Duarte, M. E. R., Cauduro, J. P., Noseda, D. G., Noseda, M. D., Gonçalves, A. G., Pujol, C. A., Damonte, E. B., & Cerezo, A. S. (2004). The structure of the agaran sulfate from Acanthophora spicifera (Rhodomelaceae, Ceramiales) and its antiviral activity. Relation between structure and antiviral activity in agarans. Carbohydrate Research, 339(2), 335–347. https://doi.org/10.1016/j.carres.2003.09.028

Eccles, R. (2020). Iota-carrageenan as an antiviral treatment for the common cold. The Open Virology Journal, 14(1), 9–15. https://doi.org/10.2174/1874357902014010009

Elizondo-Gonzalez, R., Cruz-Suarez, L. E., Ricque-Marie, D., Mendoza-Gamboa, E., Rodriguez-Padilla, C., & Trejo-Avila, L. M. (2012). In vitro characterization of the antiviral activity of fucoidan from Cladosiphon okamuranus against Newcastle Disease Virus. Virology Journal, 9(1), 307. https://doi.org/10.1186/1743-422X-9-307

El-Sekaily, A., Helal, M., & Saad, A. (2020). Enhancement of immune tolerance of COVID-19 patients might be achieved with alginate supplemented therapy. International Journal of Cancer and Biomedical Research, 4(Special Issue), 21–26. https://jcbr.journals.ekb.eg/article_92759.html

Forli, S., Huey, R., Pique, M. E., Sanner, M. F., Goodsell, D. S., & Olson, A. J. (2016). Computational protein-ligand docking and virtual drug screening with the AutoDock suite. Nature Protocols, 11(5), 905–919. https://doi.org/10.1038/nprot.2016.051

Fouchier, R. A. M., Kuiken, T., Schutten, M., van Amerongen, G., van Doornum, G. J. J., van den Hoogen, B. G., Peiris, M., Lim, W., Stöhr, K., & Osterhaus, A. D. M. E. (2003). Koch's postulates fulfilled for SARS virus. Nature, 423(6937), 240–240. https://doi.org/10.1038/423240a

Furuta, Y., Gowen, B. B., Takahashi, K., Shiraki, K., Smee, D. F., & Barnard, D. L. (2013). Favipiravir (T-705), a novel viral RNA polymerase inhibitor. Antiviral Research, 100(2), 446–454. https://doi.org/10.1016/j.antiviral.2013.09.015

Furuta, Y., Komeno, T., & Nakamura, T. (2017). Favipiravir (T-705), a broad spectrum inhibitor of viral RNA polymerase. Proceedings of the Japan Academy. Series B, Physical and Biological Sciences, 93(7), 449–463. https://doi.org/10.2183/pjab.93.027

Galili, U., Wigglesworth, K., & Abdel-Motal, U. M. (2010). Accelerated healing of skin burns by anti-Gal/α-gal liposomes interaction. Burns, 36(2), 239–251. https://doi.org/10.1016/j.burns.2009.04.002

Gantner, B. N., Simmons, R. M., Canavera, S. J., Akira, S., & Underhill, D. M. (2003). Collaborative induction of inflammatory responses by dectin-1 and toll-like receptor 2. Journal of Experimental Medicine, 197(9), 1107–1117. https://doi.org/10.1084/jem.20021787

Gaussian 09. (n.d.). Revision A. 02.

Geerlings, P., Chamorro, E., Chattaraj, P. K., De Proft, F., Gázquez, J. L., Liu, S., Morell, C., Toro-Labbé, A., Vela, A., & Ayers, P. (2020). Conceptual density functional theory: Status, prospects, issues. Theoretical Chemistry Accounts, 139(2), 36. https://doi.org/10.1007/s00214-020-2546-7

Gustafson, K. R., Cardellina, J. H., Fuller, R. W., Weislow, O. S., Kiser, R. F., Snader, K. M., Patterson, G. M. L., & Boyd, M. R. (1989). AIDS-antiviral sulfolipids from cyanobacteria (Blue-Green Algae). Journal of the National Cancer Institute , 81(16), 1254–1258. https://doi.org/10.1093/jnci/81.16.1254

Hagar, M., Ahmed, H. A., Aljohani, G., & Alhaddad, O. A. (2020). Investigation of some antiviral N-heterocycles as COVID 19 drug: Molecular docking and DFT calculations. International Journal of Molecular Sciences, 21(11), 3922. https://doi.org/10.3390/ijms21113922

Herre, J., Gordon, S., & Brown, G. D. (2004). Dectin-1 and its role in the recognition of β-glucans by macrophages. Molecular Immunology, 40(12), 869–876. https://doi.org/10.1016/j.molimm.2003.10.007

International Pharmaceutical Federation. (2020). Coronavirus SARS-CoV-2/COVID-19 pandemic: Information and Guidelines for Pharmacists and the Pharmacy Workforce.

Jayameena, P, Sivakumari, K., Ashok, K., & Rajesh, S. (2018). In Silico Molecular Docking Studies of Rutin Compound against Apoptotic Proteins (Tumor Necrosis Factor, Caspase-3, NF-Kappa-B, P53, Collagenase, Nitric Oxide Synthase and Cytochrome C). Journal of Cancer Research and Treatment, 6(2), 28–33. https://doi.org/10.12691/jcrt-6-2-1

Kang, K. A., Lee, K. H., Chae, S., Zhang, R., Jung, M. S., Ham, Y. M., Baik, J. S., Lee, N. H., & Hyun, J. W. (2006). Cytoprotective effect of phloroglucinol on oxidative stress induced cell damage via catalase activation. Journal of Cellular Biochemistry, 97(3), 609–620. https://doi.org/10.1002/jcb.20668

Kaur, R., Sharma, M., Ji, D., Xu, M., & Agyei, D. (2019). Structural features, modification, and functionalities of beta-glucan. Fibers, 8(1), 1. https://doi.org/10.3390/fib8010001

Kim, J. A., & Lee, S. B. (2016). Production of 3,6-anhydro-D-galactose from κ-carrageenan using acid catalysts. Biotechnology and Bioprocess Engineering, 21(1), 79–86. https://doi.org/10.1007/s12257-015-0636-5

Kim, K., Ehrlich, A., Perng, V., Chase, J. A., Raybould, H., Li, X., Atwill, E. R., Whelan, R., Sokale, A., & Liu, Y. (2019). Algae-derived β-glucan enhanced gut health and immune responses of weaned pigs experimentally infected with a pathogenic E. coli. Animal Feed Science and Technology, 248, 114–125. https://doi.org/10.1016/j.anifeedsci.2018.12.004

Kim, S., Chen, J., Cheng, T., Gindulyte, A., He, J., He, S., Li, Q., Shoemaker, B. A., Thiessen, P. A., Yu, B., Zaslavsky, L., Zhang, J., & Bolton, E. E. (2019). PubChem 2019 update: Improved access to chemical data. Nucleic Acids Research, 47(D1), D1102–D1109. https://doi.org/10.1093/nar/gky1033

Kirchdoerfer, R. N., & Ward, A. B. (2019). Structure of the SARS-CoV nsp12 polymerase bound to nsp7 and nsp8 co-factors. Nature Communications, 10(1), 1–9. https://doi.org/10.1038/s41467-019-10280-3

Ksiazek, T. G., Erdman, D., Goldsmith, C. S., Zaki, S. R., Peret, T., Emery, S., Tong, S., Urbani, C., Comer, J. A., Lim, W., Rollin, P. E., Dowell, S. F., Ling, A.-E., Humphrey, C. D., Shieh, W.-J., Guarner, J., Paddock, C. D., Rota, P., Fields, B., … Anderson, L. J. (2003). A novel coronavirus associated with severe acute respiratory syndrome. New England Journal of Medicine, 348(20), 1953–1966. https://doi.org/10.1056/NEJMoa030781

Lawson, C. J., & Rees, D. A. (1968). Reinvestigation of the acetolysis products of λ-carrageenan, revision of the structure of "α-1,3-gal-actotriose," and a further example of the reverse specificities of glycoside hydrolysis and acetolysis. Journal of the Chemical Society C: Organic, 1301–1304. https://doi.org/10.1039/J39680001301

Lee, S. H., Kang, S. M., Sok, C. H., Hong, J. T., Oh, J. Y., & Jeon, Y. J. (2015). Cellular activities and docking studies of eckol isolated from Ecklonia cava (Laminariales, Phaeophyceae) as potential tyrosinase

inhibitor. *Algae*, 30(2), 163–170. https://doi.org/10.4490/algae.2015.30.2.163

Liu, Q., Xu, S., Sha, Li, L., Pan, T., Ming, Shi, C., Lan., & Liu, H. (2017). In vitro and in vivo immunomodulatory activity of sulfated polysaccharide from *Porphyra haitanensis*. *Carbohydrate Polymers*, 165, 189–196. https://doi.org/10.1016/j.carbpol.2017.02.032

Lo, M. K., Feldmann, F., Gary, J. M., Jordan, R., Bannister, R., Cronin, J., Patel, N. R., Klena, J. D., Nichol, S. T., Cihlar, T., Zaki, S. R., Feldmann, H., Spiropoulou, C. F., & de Wit, E. (2019). Remdesivir (GS-5734) protects African green monkeys from Nipah virus challenge. *Science Translational Medicine*, 11(494), eaau9242. https://doi.org/10.1126/scitranslmed.aau9242

Mabeau, S., & Kloareg, B. (1987). Isolation and analysis of the cell walls of brown algae: *Fucus spiralis, F. ceranoides, F. vesiculosus, F. serratus, Bifurcaria bifurcata* and *Laminaria digitata*. *Journal of Experimental Botany*, 38(9), 1573–1580. https://doi.org/10.1093/jxb/38.9.1573

Majumdar, D., Pal, T. k., Singh, D. K., Pandey, D. K., Parai, D., Bankura, K., & Mishra, D. (2020). DFT investigations of linear Zn3-type complex with compartmental N/O-donor Schiff base: Synthesis, characterizations, crystal structure, fluorescence and molecular docking. *Journal of Molecular Structure*, 1209, 127936. https://doi.org/10.1016/j.molstruc.2020.127936

Marra, M. A., Jones, S. J. M., Astell, C. R., Holt, R. A., Brooks-Wilson, A., & Butterfield, Y. S. N. (2003). The genome sequence of the SARS-associated coronavirus. *Science*, 300(5624), 1399–1404. https://doi.org/10.1126/science.1085953

Mayer, A. M. S., Rodríguez, A. D., Taglialatela-Scafati, O., & Fusetani, N. (2013). Marine pharmacology in 2009-2011: Marine compounds with antibacterial, antidiabetic, antifungal, anti-inflammatory, antiprotozoal, antituberculosis, and antiviral activities; affecting the immune and nervous systems, and other miscellaneous mechanisms of action. *Marine Drugs*, 11(7), 2510–2573. https://doi.org/10.3390/md11072510

Meena, D. K., Das, P., Kumar, S., Mandal, S. C., Prusty, A. K., Singh, S. K., Akhtar, M. S., Behera, B. K., Kumar, K., Pal, A. K., & Mukherjee, S. C. (2013). B-glucan: An ideal immunostimulant in aquaculture (a review). *Fish Physiology and Biochemistry*, 39(3), 431–457. https://doi.org/10.1007/s10695-012-9710-5

Minari, M. C., Rincão, V. P., Soares, S. A., Ricardo, N. M. P. S., Nozawa, C., & Linhares, R. E. C. (2011). Antiviral properties of polysaccharides from *Agaricus brasiliensis* in the replication of bovine herpesvirus 1. *Acta Virologica*, 55(3), 255–259. https://doi.org/10.4149/av_2011_03_255

Morris, G. M., Huey, R., Lindstrom, W., Sanner, M. F., Belew, R. K., Goodsell, D. S., & Olson, A. J. (2009). Autodock4 and AutoDockTools4: Automated docking with selective receptor flexibility. *Journal of Computational Chemistry*, 30(16), 2785–2791. https://doi.org/10.1002/jcc.21256

Moura, A. P. V., Santos, L. C. B., Brito, C. R. N., Valencia, E., Junqueira, C., Filho, A. A. P., Sant'Anna, M. R. V., Gontijo, N. F., Bartholomeu, D. C., Fujiwara, R. T., Gazzinelli, R. T., McKay, C. S., Sanhueza, C. A., Finn, M. G., & Marques, A. F. (2017). Virus-like particle display of the α-gal carbohydrate for vaccination against Leishmania infection. *ACS Central Science*, 3(9), 1026–1031. https://doi.org/10.1021/acscentsci.7b00311

NIH. (2020). Phase 3 Efficacy and Safety Study of Favipiravir for Treatment of Uncomplicated Influenza in Adults - T705US316. Retrieved June 24, 2020, from https://clinicaltrials.gov/ct2/show/NCT02026349

O°Neill, A. N. (1955). Derivatives of 4-O-β-D-Galactopyranosyl-3,6-anhydro-D-galactose from k-Carrageenin. *Journal of the American Chemical Society*, 77, 6324–6326. https://doi.org/10.1021/ja01628a074

Oestereich, L., Lüdtke, A., Wurr, S., Rieger, T., Muñoz-Fontela, C., & Günther, S. (2014). Successful treatment of advanced Ebola virus infection with T-705 (favipiravir) in a small animal model. *Antiviral Research*, 105, 17–21. https://doi.org/10.1016/j.antiviral.2014.02.014

Ohta, K., Mizushima, Y., Hirata, N., Takemura, M., Sugawara, F., Matsukage, A., Yoshida, S., & Sakaguchi, K. (1998). Sulfoquinovosyldiacylglycerol, KM043, a new potent inhibitor of eukaryotic DNA polymerases and HIV-reverse transcriptase type 1 from a marine red alga, *Gigartina tenella*. *Chemical and Pharmaceutical Bulletin*, 46(4), 684–686. https://doi.org/10.1248/cpb.46.684

Paudel, P., Seong, S. H., Wu, S., Park, S., Jung, H. A., & Choi, J. S. (2019). Eckol as a potential therapeutic against neurodegenerative diseases

targeting dopamine D3/D4 receptors. *Marine Drugs*, 17(2), 108. https://doi.org/10.3390/md17020108

Peiris, J., Lai, S. T., Poon, L., Guan, Y., Yam, L., Lim, W., Nicholls, J., Yee, W., Yan, W. W., Cheung, M. T., Cheng, V., Chan, K. H., Tsang, D., Yung, R., Ng, T. K., & Yuen, K. Y. (2003). Coronavirus as a possible cause of severe acute respiratory syndrome. *The Lancet*, 361(9366), 1319–1325. https://doi.org/10.1016/S0140-6736(03)13077-2

Perlman, S., & Netland, J. (2009). Coronaviruses post-SARS: Update on replication and pathogenesis. *Nature Reviews Microbiology*, 7(6), 439–450. https://doi.org/10.1038/nrmicro2147

Plouguerné, E., de Souza, L., Sassaki, G., Cavalcanti, J., Villela Romanos, M., da Gama, B., Pereira, R., & Barreto-Bergter, E. (2013). Antiviral sulfoquinovosyldiacylglycerols (SQDGs) from the Brazilian brown seaweed *Sargassum vulgare*. *Marine Drugs*, 11(11), 4628–4640. https://doi.org/10.3390/md11114628

Raimundo, S. C., Pattathil, S., Eberhard, S., Hahn, M. G., & Popper, Z. A. (2017). β-1,3-Glucans are components of brown seaweed (Phaeophyceae) cell walls. *Protoplasma*, 254(2), 997–1016. https://doi.org/10.1007/s00709-016-1007-6[10.1007/s00709-016-1007-6]

Rizvi, S. M. D., Shakil, S., & Haneef, M. (2013). A simple click by click protocol to perform docking: AutoDock 4.2 made easy for non-bioinformaticians. *EXCLI journal*, 12, 831. https://doi.org/10.17877/DE290R-11534

Rota, P. A., Oberste, M. S., Monroe, S. S., Nix, W. A., Campagnoli, R., & Icenogle, J. P. (2003). Characterization of a novel coronavirus associated with severe acute respiratory syndrome. *Science*, 300(5624), 1394–1399. https://doi.org/10.1126/science.1085952

Schrödinger Release. (2019). *Desmond molecular dynamics system*. Schrödinger LLC.

Shirahashi, H., Murakami, N., Watanabe, M., Nagatsu, A., Sakakibara, J., Tokuda, H., Nishino, H., & Iwashima, A. (1993). Isolation and identification of anti-tumor-promoting principles from the fresh-water *Cyanobacterium phormidium* tenue. *Chemical and Pharmaceutical Bulletin*, 41(9), 1664–1666. https://doi.org/10.1248/cpb.41.1664

Shiraki, K., & Daikoku, T. (2020). Favipiravir, an anti-influenza drug against life-threatening RNA virus infections. *Pharmacology & Therapeutics*, 209, 107512. https://doi.org/10.1016/j.pharmthera.2020.107512

Singer, R., Derby, N., Rodriguez, A., Kizima, L., Kenney, J., Aravantinou, M., Chudolij, A., Gettie, A., Blanchard, J., Lifson, J. D., Piatak, M., Fernandez-Romero, J. A., Zydowsky, T. M., & Robbiani, M. (2011). The nonnucleoside reverse transcriptase inhibitor MIV-150 in Carrageenan gel prevents rectal transmission of simian/human immunodeficiency virus infection in macaques. *Journal of Virology*, 85(11), 5504–5512. https://doi.org/10.1128/JVI.02422-10

Tang, X., Wu, C., Li, X., Song, Y., Yao, X., Wu, X., Duan, Y., Zhang, H., Wang, Y., Qian, Z., Cui, J., & Lu, J. (2020). On the origin and continuing evolution of SARS-CoV-2. *National Science Review*, 7(6), 1012–1023. https://doi.org/10.1093/nsr/nwaa036

Walls, A. C., Park, Y. J., Tortorici, M. A., Wall, A., McGuire, A. T., & Veesler, D. (2020). Structure, function, and antigenicity of the SARS-CoV-2 spike glycoprotein. *Cell*, 181(2), 281–292.e6. https://doi.org/10.1016/j.cell.2020.02.058

Wang, M., Cao, R., Zhang, L., Yang, X., Liu, J., Xu, M., Shi, Z., Hu, Z., Zhong, W., & Xiao, G. (2020). Remdesivir and chloroquine effectively inhibit the recently emerged novel coronavirus (2019-nCoV) in vitro. *Cell Research*, 30(3), 269–271. https://doi.org/10.1038/s41422-020-0282-0

Wang, W., Wang, S. X., & Guan, H. S. (2012). The antiviral activities and mechanisms of marine polysaccharides: An overview. *Marine Drugs*, 10(12), 2795–2816. https://doi.org/10.3390/md10122795

Wang, Z., Xie, J., Shen, M., Nie, S., & Xie, M. (2018). Sulfated modification of polysaccharides: Synthesis, characterization and bioactivities. *Trends in Food Science & Technology*, 74, 147–157. https://doi.org/10.1016/j.tifs.2018.02.010

Weiss, S. R., & Navas-Martin, S. (2005). Coronavirus pathogenesis and the emerging pathogen severe acute respiratory syndrome coronavirus. *Microbiology and Molecular Biology Reviews*, 69(4), 635–664. https://doi.org/10.1128/MMBR.69.4.635-664.2005

WHO. (2015). WHO | Update 79 – Situation in China.

WHO. (2020a). Naming the coronavirus disease (COVID-19) and the virus that causes it. Retrieved July 2, 2020, from https://www.who.int/emergencies/diseases/novel-coronavirus-2019/technical-guidance/naming-the-coronavirus-disease-(covid-2019)-and-the-virus-that-causes-it

WHO. (2020b). Prioritizing diseases for research and development in emergency contexts. Retrieved July 4, 2020, from https://www.who.int/activities/prioritizing-diseases-for-research-and-development-in-emergency-contexts

Xianliang, X., Meiyu, G., Huashi, G., & Zelin, L. (2000). Study on the mechanism of inhibitory action of 911 on replication of HIV-1 in vitro. *Zhongguo hai Yang yao wu= Chinese Journal of Marine Drugs*, *19*(4), 15–18.

Yilmaz, B., Portugal, S., Tran, T. M., Gozzelino, R., Ramos, S., Gomes, J., Regalado, A., Cowan, P. J., d'Apice, A. J. F., Chong, A. S., Doumbo, O. K., Traore, B., Crompton, P. D., Silveira, H., & Soares, M. P. (2014). Gut microbiota elicits a protective immune response against malaria transmission. *Cell*, *159*(6), 1277–1289. https://doi.org/10.1016/j.cell.2014.10.053

Zhang, L., Lin, D., Sun, X., Curth, U., Drosten, C., Sauerhering, L., Becker, S., Rox, K., & Hilgenfeld, R. (2020). Crystal structure of SARS-CoV-2 main protease provides a basis for design of improved a-ketoamide inhibitors. *Science*, *368*(6489), 409–412. https://doi.org/10.1126/science.abb3405